Encounter-based approach to diffusion with resetting

Ziyad Benkhadaj [1] and Denis S. Grebenkov [2,*]
[1]*ENS Paris-Saclay, 91190 Gif-sur-Yvette, France*
[2]*Laboratoire de Physique de la Matière Condensée (UMR 7643), CNRS–Ecole Polytechnique, IP Paris, 91128 Palaiseau, France*

(Received 10 July 2022; accepted 27 September 2022; published 14 October 2022)

An encounter-based approach consists in using the boundary local time as a proxy for the number of encounters between a diffusing particle and a target to implement various surface reaction mechanisms on that target. In this paper, we investigate the effects of stochastic resetting onto diffusion-controlled reactions in bounded confining domains. We first discuss the effect of position resetting onto the propagator and related quantities; in this way, we retrieve a number of earlier results but also provide complementary insights into them. Second, we introduce boundary local time resetting and investigate its impact. Curiously, we find that this type of resetting does not alter the conventional propagator governing the diffusive dynamics in the presence of a partially reactive target with a constant reactivity. In turn, the generalized propagator for other surface reaction mechanisms can be significantly affected. Our general results are illustrated for diffusion on an interval with reactive end points. Further perspectives and some open problems are discussed.

DOI: 10.1103/PhysRevE.106.044121

I. INTRODUCTION

Diffusion-controlled reactions and the related first-passage phenomena are ubiquitous in nature and industrial applications [1–6]. In a typical setting, a particle (e.g., a ligand) diffuses towards a specific location in a confining environment (e.g., a cytoplasm) and attempts to bind to or react on that target (e.g., a receptor). The macroscopic concentration of particles or, equivalently, the survival probability of a single particle satisfies a Fokker-Planck equation with appropriate boundary conditions. Since the seminal paper by von Smoluchowski [7], diffusion-controlled reactions have been thoroughly investigated to reveal the respective roles of the structural complexity of the environment, of the diffusive dynamics in the bulk, of the location, shape, size, and reactivity of the target, etc. [8–24].

Evans and Majumdar have introduced a new aspect into this field—stochastic resetting, according to which the particle can be spontaneously relocated into its initial position to restart diffusion towards the target [25]. Such resetting steps allow the particle to abandon its original random path that could be too long or even might never lead to the target. For instance, if the particle diffuses on the positive half-line towards the origin, the mean first-passage time (FPT) to that target is infinite due to contributions of too long paths. In turn, resetting prohibits long paths and renders the mean FPT finite. This basic example reveals that resetting can be beneficial for diffusive search and lead to a variety of optimization problems. We emphasize that this resetting mechanism is independent of the diffusive dynamics and is thus different from the instantaneous return process [26] and its extensions (see [27–32] and references therein), in which the process is reset to a random bulk point after hitting the boundary or crossing a given threshold.

Since its introduction in 2011, various effects of stochastic resetting onto diffusion-controlled reactions and related first-passage times have been studied. For instance, Evans *et al.* extended the above basic setting to deal with a space-dependent resetting rate, resetting to a random position drawn from a resetting distribution, a spatial distribution for the absorbing target [33], partial reactivity of the target, the effect of multiple searchers [34], and Lévy flights [35] (see also [36]). Pal *et al.* focused on the time-dependent resetting rate and determined the survival probability under resetting and optimal resetting rate function [37]. Reuveni showed that the relative standard deviation associated with the FPT of an optimally restarted process (with a constant rate) was always equal to 1, independently of the dynamics [38]. A relation to the Michaelis-Menten reaction scheme [39] was also discussed. Pal and Reuveni proposed an elegant general approach to analyze the effect of resetting with an arbitrarily distributed resetting time δ onto the statistics of any first-passage time $\mathcal{T}$ [40]. In particular, they deduced a simple formula for the mean value of the FPT $\mathcal{T}_\phi$ under resetting:

$$\mathbb{E}\{\mathcal{T}_\phi\} = \frac{\mathbb{E}\{\min\{\mathcal{T},\delta\}\}}{\mathbb{P}\{\mathcal{T}<\delta\}}, \tag{1}$$

where $\mathbb{E}\{\cdot\}$ denotes the expectation. This approach was further elaborated by Chechkin and Sokolov [41] into a general renewal scheme that we will employ in this paper. They derived another representation for $\mathbb{E}\{\mathcal{T}_\phi\}$ to investigate the search optimality under resetting [see Eq. (27) and the related discussion below]. The effect of refractory period on stochastic resetting was investigated in [42]. In the case of continuous-time random walks with power-law distributed waiting times between jumps, long-range memory effects can be considerably altered by resetting [43], leading to peculiar behaviors of the

*denis.grebenkov@polytechnique.edu

 ©2022 American Physical Society

propagator and the mean-squared displacement (MSD) of the particle (see also [44] for other insights into the MSD). Dahlenburg *et al.* introduced random-amplitude stochastic resetting, in which the diffusing particle may be only partially reset towards the origin or even overshoot the origin in a resetting step [45]. The role of a bias due to a potential onto the search optimality under resetting was analyzed [46,47]. In the case of Poissonian resetting, one can go beyond the propagator and the first-passage time distribution and investigate additive functionals of a stochastic process, e.g., its residence time. Meylahn *et al.* considered Markov processes with resetting and derived the rate function of additive functionals characterizing the likelihood of their fluctuations in the long-time limit [48] (see also [49,50]). Finally, an experimental realization of colloidal particle diffusion with resetting via holographic optical tweezers was reported [51]. This work permitted to measure the energetic cost of resetting and to reveal the need for some improvements in theoretical analysis to account for fundamental constraints on realistic resetting protocols. These and many other aspects of stochastic resetting have been recently reviewed [52]. Even though the renewal approach is valid for rather general diffusive processes, most former works focused on one-dimensional diffusion on a line or a half-line, while extensions to higher dimensions concerned the whole space $\mathbb{R}^d$. In particular, the specific effects related to restricted diffusion in bounded domains have not been explored yet.

In this paper, we propose to look at the role of stochastic resetting in the so-called encounter-based approach to diffusion-mediated surface phenomena [53]. This approach is based on the concept of the *boundary local time* ℓ_t, which quantifies the number of encounters between the diffusing particle and the boundary up to time t. The diffusive dynamics is entirely characterized by the full propagator $P(\boldsymbol{x}, \ell, t|\boldsymbol{x}_0)$—the joint probability density of the particle position $\boldsymbol{X}_t$ and its boundary local time ℓ_t at time t, given that the particle started from a point $\boldsymbol{x}_0$ at time 0. Once the full propagator is determined for a passive (nonreactive) boundary, different surface reaction mechanisms can be implemented (see Sec. II A). In this way, one can retrieve the conventional constant reactivity described by the Robin boundary condition as a specific model, one among many others. Several extensions and applications of the encounter-based approach have been recently discussed [53–61]. Here, we aim at investigating the role of resetting within this paradigm.

Importantly, the encounter-based approach offers more flexibility on the implementation of resetting (Fig. 1). On the one hand, one can keep the boundary local time as a history of encounters with the boundary while resetting the position of the particle, as done in former studies. In this direction, one should be able to retrieve former results but also discover new ones, e.g., the distribution of the boundary local time or correlations between $\boldsymbol{X}_t$ and ℓ_t. On the other hand, the particle trajectory can be kept unchanged while resetting the boundary local time. This is a new resetting scheme, which can model some reactivity dynamics of the target. Such features were not available within the conventional description of diffusion-controlled reactions that focused exclusively on the position of the particle. Finally, one can consider even more sophisticated

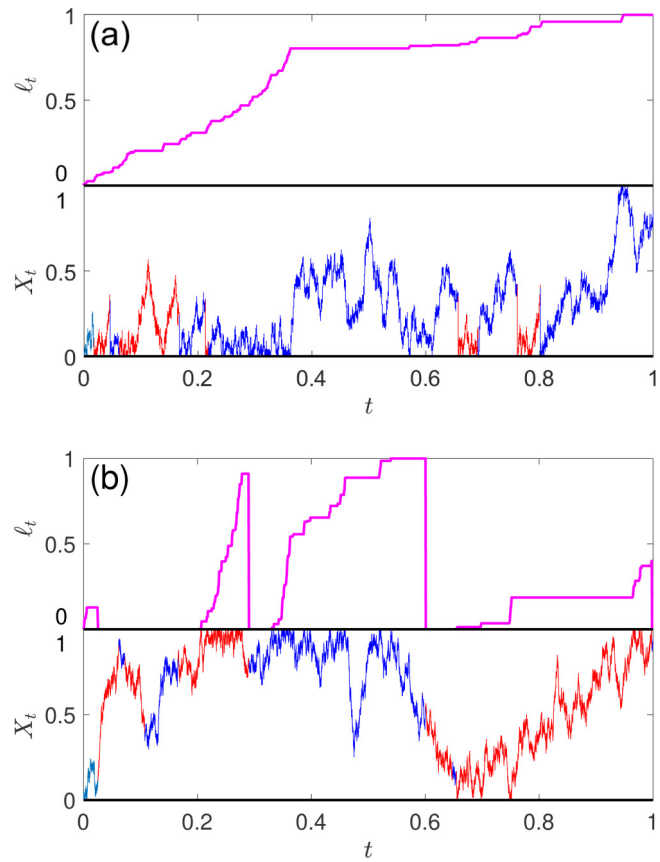

FIG. 1. Simulation of a random trajectory X_t on the unit interval (0,1) and its boundary local time ℓ_t under Poissonian resetting with the law $\mathbb{P}\{\delta > t\} = \Phi(t) = e^{-\omega t}$ for the resetting time δ, with the rate $\omega = 10$, the diffusion coefficient $D = 1$, and the starting point $x_0 = 0$. The boundary local time is rescaled by its maximum and shifted upwards for an easier visualization. (a) Position resetting; (b) boundary local time resetting. The trajectory is shown by pieces that change color (blue and red) at each resetting.

resetting mechanisms that involve both the position $\boldsymbol{X}_t$ of the particle and its boundary local time ℓ_t.

The paper is organized as follows. Section II presents our main results in general bounded domains. We start in Sec. II A by recalling the encounter-based approach and summarizing the main notations and formulas that will be used in the paper. In Sec. II B, we derive the full propagator and related quantities under resetting of the position, whereas Sec. II C is devoted to resetting of the boundary local time. In Sec. III, we illustrate general results in the case of diffusion on an interval, for which most quantities can be found explicitly. Section IV summarizes our results and presents further perspectives.

II. GENERAL RESULTS

A. Encounter-based approach

We consider a pointlike particle diffusing with a constant diffusivity D in a bounded Euclidean domain $\Omega \subset \mathbb{R}^d$ with a smooth reflecting boundary $\partial\Omega$. For a particle started at time 0 from a point $\boldsymbol{x}_0 \in \Omega$, the stochastic process $\boldsymbol{X}_t$ denotes its (random) position at time t. We are interested in describing surface reactions on a chosen "target" Γ, which is a subset

of the otherwise inert boundary $\partial\Omega$. Following Lévy, one can introduce the boundary local time ℓ_t on Γ as [62–64]

$$\ell_t = \lim_{a\to 0} \frac{D}{a} \underbrace{\int_0^t dt'\, \Theta(a - |\boldsymbol{X}_{t'} - \Gamma|)}_{\text{residence time in } \Gamma_a}, \tag{2}$$

where $|\boldsymbol{x} - \Gamma|$ is the Euclidean distance between a point $\boldsymbol{x}$ and the target set Γ, and $\Theta(z)$ is the Heaviside step function: $\Theta(z) = 1$ for $z > 0$ and 0 otherwise. Here the integral over t' is the residence time of the particle inside a thin boundary layer $\Gamma_a = \{\boldsymbol{x} \in \Omega : |\boldsymbol{x} - \Gamma| < a\}$ of width a near the target [defined via $\Theta(a - |\boldsymbol{X}_{t'} - \Gamma|)$]. As the target Γ has a lower dimensionality $d - 1$ as compared to the confining domain Ω, the residence time vanishes in the limit $a \to 0$. In turn, its rescaling by a yields a well-defined limit. Even though ℓ_t is called "boundary local time," it has units of length (in turn, ℓ_t/D has units of time per length). We stress that the mathematical construction of reflected Brownian motion via the stochastic Skorokhod equation involves the boundary local time on the whole boundary $\partial\Omega$. Here, we consider its modified version by restricting the residence time in Eq. (2) to the subset Γ, which represents a target. Accordingly, we introduce the full propagator $P(\boldsymbol{x}, \ell, t|\boldsymbol{x}_0)$ as the joint probability density of the particle position $\boldsymbol{X}_t$ inside Ω and its boundary local time ℓ_t *on the target*. We also outline that the *boundary* local time should be distinguished from a *point* local time, which represents the rescaled residence time in the vicinity of a bulk point. The latter has been studied intensively (see [65–67] and references therein), in particular in the context of stochastic resetting [68]. For this purpose, one could use the Feynman-Kac formula with δ-shaped potential in the bulk. However, the application of this formula to the boundary local time would require setting singular δ-potentials on the boundary that renders the whole approach less appealing (see Sec. E of the supplemental material of [53] for further discussions). For this reason, the analysis of the boundary local time relies on different mathematical tools discussed below.

In many physical, chemical, and biological applications, the target Γ can be modeled as a thin reactive layer Γ_a with some bulk reactivity rate μ (in units 1/s). When the layer width a is small, the definition (2) indicates that $a\ell_t/D$ characterizes the residence time that a particle has spent in the reactive layer, up to time t. For a basic first-order reaction kinetics, the survival probability of the particle $S_q(t|\boldsymbol{x}_0)$ (i.e., the probability that the particle has not reacted in Γ_a up to time t) is then

$$S_q(t|\boldsymbol{x}_0) = \mathbb{E}\{e^{-\mu a \ell_t/D}\}, \tag{3}$$

where

$$q = \frac{\mu a}{D} = \frac{\kappa}{D}, \tag{4}$$

with $\kappa = \mu a$ being the target reactivity (in units m/s). By introducing an independent random variable $\hat{\ell}$ with an exponential law, $\mathbb{P}\{\hat{\ell} > \ell\} = e^{-q\ell}$, one can rewrite the above expectation as [53]

$$S_q(t|\boldsymbol{x}_0) = \mathbb{P}\{\ell_t < \hat{\ell}\} = \int_0^\infty d\ell \underbrace{e^{-q\ell}}_{=\mathbb{P}\{\ell<\hat{\ell}\}} \rho(\ell, t|\boldsymbol{x}_0), \tag{5}$$

where

$$\rho(\ell, t|\boldsymbol{x}_0) = \int_\Omega d\boldsymbol{x}\, P(\boldsymbol{x}, \ell, t|\boldsymbol{x}_0) \tag{6}$$

is the probability density of the boundary local time ℓ_t [here and throughout the text, the real positive variable ℓ in $\rho(\ell, t|\boldsymbol{x}_0)$ and related expressions denotes any possible realization of the random variable ℓ_t]. In this representation, the reaction on the target Γ occurs at the first time when the boundary local time ℓ_t exceeds the random threshold $\hat{\ell}$ that naturally defines the first-reaction time (FRT) $\mathcal{T}$ as

$$\mathcal{T} = \inf\{t > 0 : \ell_t > \hat{\ell}\}. \tag{7}$$

As the boundary local time ℓ_t is a nondecreasing process, one has $S_q(t|\boldsymbol{x}_0) = \mathbb{P}\{\ell_t < \hat{\ell}\} = \mathbb{P}\{\mathcal{T} > t\}$ so that the survival probability determines the cumulative distribution function of the first-reaction time $\mathcal{T}$, its probability density,

$$H_q(t|\boldsymbol{x}_0) = -\partial_t S_q(t|\boldsymbol{x}_0), \tag{8}$$

and all the moments. Moreover, as the threshold $\hat{\ell}$ is exponentially distributed, one can express $H_q(t|\boldsymbol{x}_0)$ as

$$H_q(t|\boldsymbol{x}_0) = \int_0^\infty d\ell \underbrace{q e^{-q\ell}}_{=\text{pdf of } \hat{\ell}} U(\ell, t|\boldsymbol{x}_0), \tag{9}$$

where $U(\ell, t|\boldsymbol{x}_0)$ is the probability density of the first-crossing time $\mathcal{T}_\ell$ of a fixed threshold ℓ by ℓ_t:

$$\mathcal{T}_\ell = \inf\{t > 0 : \ell_t > \ell\}. \tag{10}$$

In analogy with Eq. (5), one can relate the full propagator $P(\boldsymbol{x}, \ell, t|\boldsymbol{x}_0)$ to the conventional propagator $G_q(\boldsymbol{x}, t|\boldsymbol{x}_0)$ as [53]

$$G_q(\boldsymbol{x}, t|\boldsymbol{x}_0) = \int_0^\infty d\ell\, e^{-q\ell} P(\boldsymbol{x}, \ell, t|\boldsymbol{x}_0). \tag{11}$$

Note that the integral of this relation over $\boldsymbol{x} \in \Omega$ yields Eq. (5). Here, the full propagator $P(\boldsymbol{x}, \ell, t|\boldsymbol{x}_0)$ describes the diffusive dynamics inside the confining domain Ω with a reflecting inert boundary $\partial\Omega$, i.e., *without any surface reaction*, even on the target region Γ. In turn, the conventional propagator $G_q(\boldsymbol{x}, t|\boldsymbol{x}_0)$ describes the probability density of finding the particle at time t in the vicinity of point $\boldsymbol{x}$ in the presence of partially reactive target Γ with reactivity parameter q, thus accounting for the survival of the particle. One sees that the effect of surface reactions on the target Γ is incorporated *a posteriori* via the factor $e^{-q\ell}$. Moreover, one can replace the exponential law $e^{-q\ell}$ for the random threshold $\hat{\ell}$ by any law, $\mathbb{P}\{\hat{\ell} > \ell\} = \Psi(\ell)$, that defines a generalized propagator

$$G_\Psi(\boldsymbol{x}, t|\boldsymbol{x}_0) = \int_0^\infty d\ell\, \Psi(\ell) P(\boldsymbol{x}, \ell, t|\boldsymbol{x}_0), \tag{12}$$

and allows one to deal with more sophisticated surface reaction mechanisms [53].

We outline the explicit dependence on q in Eq. (11), in contrast to the conventional descriptions [69–88], in which the parameter q enters *implicitly* through the Robin boundary condition to the diffusion equation:

$$\partial_t G_q(\boldsymbol{x}, t|\boldsymbol{x}_0) = D\Delta G_q(\boldsymbol{x}, t|\boldsymbol{x}_0) \quad (\boldsymbol{x} \in \Omega), \tag{13a}$$

$$-\partial_n G_q(\boldsymbol{x}, t|\boldsymbol{x}_0) = q G_q(\boldsymbol{x}, t|\boldsymbol{x}_0) \quad (\boldsymbol{x} \in \Gamma), \tag{13b}$$

$$-\partial_n G_q(\boldsymbol{x}, t|\boldsymbol{x}_0) = 0 \quad (\boldsymbol{x} \in \partial\Omega\backslash\Gamma), \tag{13c}$$

subject to the initial condition $G_q(\boldsymbol{x}, t=0|\boldsymbol{x}_0) = \delta(\boldsymbol{x}-\boldsymbol{x}_0)$ with the Dirac distribution. Here Δ is the Laplace operator and ∂_n is the normal derivative oriented outwards the domain Ω. As stressed in [53], the Robin boundary condition (13b), which is consistent with the exponential model (3) of the survival probability, is a *choice* of one surface reaction mechanism among many others.

As the domain Ω is bounded, the Laplace operator has a discrete spectrum, and the solution of the above equations can be expressed via a spectral decomposition

$$G_q(\boldsymbol{x}, t|\boldsymbol{x}_0) = \sum_{k=0}^{\infty} u_k^{(q)}(\boldsymbol{x}) \left[u_k^{(q)}(\boldsymbol{x}_0)\right]^* e^{-Dt\lambda_k^{(q)}}, \tag{14}$$

where the asterisk denotes complex conjugate, while $\lambda_k^{(q)}$ and $u_k^{(q)}(\boldsymbol{x})$ are the eigenvalues and $L_2(\Omega)$-normalized eigenfunctions of the (negative) Laplace operator $-\Delta$ in Ω:

$$-\Delta u_k^{(q)}(\boldsymbol{x}) = \lambda_k^{(q)} u_k^{(q)}(\boldsymbol{x}) \quad (\boldsymbol{x} \in \Omega), \tag{15a}$$

$$-\partial_n u_k^{(q)}(\boldsymbol{x}) = q u_k^{(q)}(\boldsymbol{x}) \quad (\boldsymbol{x} \in \Gamma), \tag{15b}$$

$$-\partial_n u_k^{(q)}(\boldsymbol{x}) = 0 \quad (\boldsymbol{x} \in \partial\Omega\backslash\Gamma). \tag{15c}$$

The spectral expansion (14) highlights the symmetry of the propagator with respect to the exchange of the starting and arrival points $\boldsymbol{x}_0$ and $\boldsymbol{x}$: $G_q(\boldsymbol{x}, t|\boldsymbol{x}_0) = G_q(\boldsymbol{x}_0, t|\boldsymbol{x})$. The spectral expansion of the full propagator, derived in [53], implies the same symmetry,

$$P(\boldsymbol{x}, \ell, t|\boldsymbol{x}_0) = P(\boldsymbol{x}_0, \ell, t|\boldsymbol{x}). \tag{16}$$

Such a symmetry can be broken in the presence of a drift or a potential (see [58] for details).

In the following, we describe how resetting may affect the above quantities: the full propagator $P(\boldsymbol{x}, \ell, t|\boldsymbol{x}_0)$, the conventional propagator $G_q(\boldsymbol{x}, t|\boldsymbol{x}_0)$, and the probability densities $\rho(\ell, t|\boldsymbol{x}_0)$, $H_q(t|\boldsymbol{x}_0)$, and $U(\ell, t|\boldsymbol{x}_0)$ of the boundary local time ℓ_t, of the first-reaction time $\mathcal{T}$, and of the first-crossing time $\mathcal{T}_\ell$, respectively.

B. Position resetting

We start by looking at the conventional scenario of stochastic resetting of the particle position. At each resetting, the particle is immediately relocated to its starting position $\boldsymbol{x}_0$. We assume that durations δ_1, δ_2, etc. between consecutive resettings are independent identically distributed random variables drawn from a prescribed probability density function (PDF) $\phi(t)$. In other words, resettings occur at random times $t_1 = \delta_1, t_2 = \delta_1 + \delta_2, \ldots, t_k = \delta_1 + \cdots + \delta_k$, etc. We first present general results and then discuss the Poissonian resetting with a rate ω [i.e., $\phi(t) = \omega e^{-\omega t}$] as one of the most common models of stochastic resetting. Note that the Poissonian case was recently studied in [61] (see also Sec. IV).

1. General results

Following and extending the renewal approach from [41] (see also [42,52,89]), we compute the full propagator with resetting, denoted as $P_\phi(\boldsymbol{x}, \ell, t|\boldsymbol{x}_0)$, by counting the number of resettings up to time t and adding their contributions:

$$\begin{aligned} P_\phi(\boldsymbol{x}, \ell, t|\boldsymbol{x}_0) &= \Phi(t)P(\boldsymbol{x}, \ell, t|\boldsymbol{x}_0) + \int_0^t dt_1 \phi(t_1) \int_\Omega \int_0^\ell d\boldsymbol{x}_1 d\ell_1 P(\boldsymbol{x}_1, \ell_1, t_1|\boldsymbol{x}_0)\, \Phi(t-t_1) P(\boldsymbol{x}, \ell-\ell_1, t-t_1|\boldsymbol{x}_0) \\ &\quad + \int_0^t dt_1 \phi(t_1) \int_\Omega \int_0^\ell d\boldsymbol{x}_1 d\ell_1 P(\boldsymbol{x}_1, \ell_1, t_1|\boldsymbol{x}_0) \int_0^{t-t_1} dt_2 \phi(t_2) \int_\Omega \int_0^{\ell-\ell_1} d\boldsymbol{x}_2 d\ell_2 P(\boldsymbol{x}_2, \ell_2, t_2|\boldsymbol{x}_0) \\ &\quad \times \Phi(t-t_1-t_2) P(\boldsymbol{x}, \ell-\ell_1-\ell_2, t-t_1-t_2|\boldsymbol{x}_0) + \cdots, \end{aligned} \tag{17}$$

where $\Phi(t) = \int_t^\infty dt' \phi(t')$ is the probability of no resetting up to time t. The first term is the contribution without resetting. The second term describes one resetting at time t_1 [with probability $\phi(t_1)dt_1$], which can range from 0 to t. The factor $P(\boldsymbol{x}_1, \ell_1, t_1|\boldsymbol{x}_0)d\boldsymbol{x}_1 d\ell_1$ describes the probability for the particle to be at an intermediate position $\boldsymbol{x}_1$ with an intermediate boundary local time ℓ_1. After resetting, the position of the particle is reset to $\boldsymbol{x}_0$ while the boundary local time remains unchanged. The Markov property implies that the remaining part of the diffusive process, from t_1 to t, is described by the probability density $P(\boldsymbol{x}, \ell-\ell_1, t-t_1|\boldsymbol{x}_0)$, while $\Phi(t-t_1)$ ensures that there is no resetting during that period. Similarly, the third, fourth, etc. terms describe the contributions of two, three, etc. resettings. Note that one can easily implement the case when the resetting position is different from the starting point $\boldsymbol{x}_0$.

Using the probability density $\rho(\ell, t|\boldsymbol{x}_0)$ of the boundary local time ℓ_t defined by Eq. (6), one can simplify the integrals over intermediate positions $\boldsymbol{x}_1$, $\boldsymbol{x}_2$, etc. In turn, the convolutions over ℓ_k and t_k can be turned into products by performing the double Laplace transform with respect to variables ℓ and t that is defined for a given function $f(\ell, t)$ as

$$\mathcal{L}_{q,p}\{f(\ell, t)\} = \int_0^\infty d\ell\, e^{-q\ell} \int_0^\infty dt\, e^{-pt} f(\ell, t). \tag{18}$$

Applying this transform to Eq. (17) and summing the resulting geometric series, one has

$$\mathcal{L}_{q,p}\{P_\phi(\boldsymbol{x}, \ell, t|\boldsymbol{x}_0)\} = \frac{\mathcal{L}_{q,p}\{\Phi(t)P(\boldsymbol{x}, \ell, t|\boldsymbol{x}_0)\}}{1 - \mathcal{L}_{q,p}\{\phi(t)\rho(\ell, t|\boldsymbol{x}_0)\}}. \tag{19}$$

As $\Phi(t)$ and $\phi(t)$ do not depend on ℓ, one can first perform the Laplace transform with respect to ℓ to get

$$\mathcal{L}_{q,p}\{P_\phi(\boldsymbol{x},\ell,t|\boldsymbol{x}_0)\} = \frac{\mathcal{L}_p\{\Phi(t)G_q(\boldsymbol{x},t|\boldsymbol{x}_0)\}}{1-\mathcal{L}_p\{\phi(t)S_q(t|\boldsymbol{x}_0)\}}, \tag{20}$$

where we used Eqs. (5) and (11), and $\mathcal{L}_p$ denotes the Laplace transform with respect to t. An inversion of the double Laplace transform in this equation formally yields the full propagator $P_\phi(\boldsymbol{x},\ell,t|\boldsymbol{x}_0)$ under resetting:

$$P_\phi(\boldsymbol{x},\ell,t|\boldsymbol{x}_0) = \mathcal{L}_{q,p}^{-1}\left\{\frac{\mathcal{L}_p\{\Phi(t)G_q(\boldsymbol{x},t|\boldsymbol{x}_0)\}}{1-\mathcal{L}_p\{\phi(t)S_q(t|\boldsymbol{x}_0)\}}\right\}, \tag{21}$$

where $\mathcal{L}_{q,p}^{-1}$ denotes the double inverse Laplace transform with respect to q and p. This expression outlines that position resetting breaks the symmetry of the full propagator with respect to the exchange between $\boldsymbol{x}$ and $\boldsymbol{x}_0$, in sharp contrast to Eq. (16) for the full propagator $P(\boldsymbol{x},\ell,t|\boldsymbol{x}_0)$ without resetting. This is not surprising, because resetting to the starting point $\boldsymbol{x}_0$ distinguishes it from other points. Expectedly, the form of Eq. (20) resembles Eq. (1) from [41] for the probability density of the first-passage time. However, Eq. (20) gives access to more refined information about the diffusing particle—to its full propagator under resetting.

In analogy with Eq. (11), the Laplace transform of $P_\phi(\boldsymbol{x},\ell,t|\boldsymbol{x}_0)$ with respect to ℓ determines the conventional propagator under resetting that we denote as $G_{q,\phi}(\boldsymbol{x},t|\boldsymbol{x}_0)$. In other words, Eq. (20) can be written as

$$\tilde{G}_{q,\phi}(\boldsymbol{x},p|\boldsymbol{x}_0) = \frac{\mathcal{L}_p\{\Phi(t)G_q(\boldsymbol{x},t|\boldsymbol{x}_0)\}}{1-\mathcal{L}_p\{\phi(t)S_q(t|\boldsymbol{x}_0)\}}, \tag{22}$$

where the tilde denotes the Laplace transform $\mathcal{L}_p$ of $G_{q,\phi}(\boldsymbol{x},t|\boldsymbol{x}_0)$ with respect to time t (we keep using this tilde notation for other quantities in the following). The inverse Laplace transform formally yields the propagator under resetting in the time domain:

$$G_{q,\phi}(\boldsymbol{x},t|\boldsymbol{x}_0) = \mathcal{L}_p^{-1}\left\{\frac{\mathcal{L}_p\{\Phi(t)G_q(\boldsymbol{x},t|\boldsymbol{x}_0)\}}{1-\mathcal{L}_p\{\phi(t)S_q(t|\boldsymbol{x}_0)\}}\right\}. \tag{23}$$

For a reactive target ($q>0$), the propagator $G_{q,\phi}(\boldsymbol{x},t|\boldsymbol{x}_0)$ is expected to vanish in the long-time limit, as the particle diffusing in a bounded domain cannot in general avoid hitting the target (see the discussion below in the case of a Poissonian resetting). In turn, if the target is inert ($q=0$), the particle survives forever, $S_0(t|\boldsymbol{x}_0)=1$, whereas the conventional propagator approaches a steady-state uniform distribution: $G_0(\boldsymbol{x},t|\boldsymbol{x}_0)\to 1/|\Omega|$ as $t\to\infty$, where $|\Omega|$ is the volume of the confining domain Ω. If the resetting time density $\phi(t)$ has a finite mean $\mathbb{E}\{\delta\}$, the denominator of Eq. (23) behaves in the small-p limit as $1-\mathcal{L}_p\{\phi(t)S_0(t|\boldsymbol{x}_0)\} = 1-\tilde{\phi}(p)\approx p\mathbb{E}\{\delta\}+O(p^2)$, which implies the long-time behavior

$$G_{0,\phi}(\boldsymbol{x},t|\boldsymbol{x}_0) \xrightarrow{t\to\infty} G_{0,\phi}^{\rm st}(\boldsymbol{x}|\boldsymbol{x}_0) = \int_0^\infty \frac{dt\,\Phi(t)}{\mathbb{E}\{\delta\}} G_0(\boldsymbol{x},t|\boldsymbol{x}_0). \tag{24}$$

When there was no resetting, the diffusing particle explored the bounded confining domain and therefore equilibrated the likelihood of its location at any point in Ω (the uniform steady-state distribution). Moreover, the information on the starting point was lost. In contrast, resetting breaks this uniformity and preserves information on the resetting point in the steady-state distribution $G_{0,\phi}^{\rm st}(\boldsymbol{x}|\boldsymbol{x}_0)$.

The integral of the propagator in Eq. (23) over $\boldsymbol{x}\in\Omega$ determines the survival probability under resetting:

$$S_{q,\phi}(t|\boldsymbol{x}_0) = \mathcal{L}_p^{-1}\left\{\frac{\mathcal{L}_p\{\Phi(t)S_q(t|\boldsymbol{x}_0)\}}{1-\mathcal{L}_p\{\phi(t)S_q(t|\boldsymbol{x}_0)\}}\right\}, \tag{25}$$

or, equivalently,

$$\tilde{S}_{q,\phi}(p|\boldsymbol{x}_0) = \frac{\mathcal{L}_p\{\Phi(t)S_q(t|\boldsymbol{x}_0)\}}{1-\mathcal{L}_p\{\phi(t)S_q(t|\boldsymbol{x}_0)\}}. \tag{26}$$

As previously, the survival probability determines the probability density $H_{q,\phi}(t|\boldsymbol{x}_0) = -\partial_t S_{q,\phi}(t|\boldsymbol{x}_0)$ of the first-reaction time $\mathcal{T}_\phi$ under resetting, as well as its moments. In particular, the mean FRT under resetting is

$$\begin{aligned}\mathbb{E}\{\mathcal{T}_\phi\} &= \int_0^\infty dt\,t\,H_{q,\phi}(t|\boldsymbol{x}_0) = \int_0^\infty dt\,S_{q,\phi}(t|\boldsymbol{x}_0)\\ &= \tilde{S}_{q,\phi}(0|\boldsymbol{x}_0) = \frac{\int_0^\infty dt\,\Phi(t)\,S_q(t|\boldsymbol{x}_0)}{\int_0^\infty dt\,\Phi(t)\,H_q(t|\boldsymbol{x}_0)},\end{aligned} \tag{27}$$

where we used that $\phi(t) = -\partial_t\Phi(t)$, Eq. (8), and integrated by parts in the denominator. This expression was earlier derived by Pal *et al.* [37], as well as by Chechkin and Sokolov [41], who used it to investigate the search optimality under resetting (see also [52]). Note that Eq. (27) is equivalent to the general form (1) obtained by Pal and Reuveni [40]. We also note that the relation (9), which is valid under position resetting, can be inverted to access the probability density of the first-crossing time under resetting:

$$U_\phi(\ell,t|\boldsymbol{x}_0) = \mathcal{L}_{q,p}^{-1}\left\{\frac{\tilde{H}_{q,\phi}(p|\boldsymbol{x}_0)}{q}\right\}. \tag{28}$$

Finally, the integral of Eq. (21) over $\boldsymbol{x}\in\Omega$ yields the probability density $\rho_\phi(\ell,t|\boldsymbol{x}_0)$ of the boundary local time under resetting:

$$\rho_\phi(\ell,t|\boldsymbol{x}_0) = \mathcal{L}_{q,p}^{-1}\left\{\frac{\mathcal{L}_p\{\Phi(t)S_q(t|\boldsymbol{x}_0)\}}{1-\mathcal{L}_p\{\phi(t)S_q(t|\boldsymbol{x}_0)\}}\right\}. \tag{29}$$

2. Poissonian resetting

For the Poissonian resetting with $\Phi(t)=e^{-\omega t}$, we use again Eq. (11) to simplify Eq. (22) as

$$\tilde{G}_{q,\omega}(\boldsymbol{x},p|\boldsymbol{x}_0) = \frac{\tilde{G}_q(\boldsymbol{x},p+\omega|\boldsymbol{x}_0)}{1-\omega\tilde{S}_q(p+\omega|\boldsymbol{x}_0)}. \tag{30}$$

One can invert this Laplace transform via the residue theorem by finding the poles $\{p_k\}\subset\mathbb{C}$ of $\tilde{G}_{q,\omega}(\boldsymbol{x},p|\boldsymbol{x}_0)$. For $q>0$, these poles are determined by the equation

$$\tilde{S}_q(p_k+\omega|\boldsymbol{x}_0) = \frac{1}{\omega}. \tag{31}$$

In the limit $\omega\to 0$, the resetting is progressively switched off, and the kth pole p_k approaches $-D\lambda_k^{(q)}$. The pole p_0 with the largest real part determines the exponential decay of the propagator $G_{q,\omega}(\boldsymbol{x},t|\boldsymbol{x}_0)$ in the long-time limit.

In turn, for the inert target ($q=0$), Eq. (30) simplifies to

$$\tilde{G}_{0,\omega}(\boldsymbol{x},p|\boldsymbol{x}_0) = \left(1+\frac{\omega}{p}\right)\tilde{G}_0(\boldsymbol{x},p+\omega|\boldsymbol{x}_0), \tag{32}$$

which in the time domain reads

$$G_{0,\omega}(\boldsymbol{x}, t|\boldsymbol{x}_0) = e^{-\omega t} G_0(\boldsymbol{x}, t|\boldsymbol{x}_0) + \omega \int_0^t dt' e^{-\omega t'} G_0(\boldsymbol{x}, t'|\boldsymbol{x}_0). \quad (33)$$

This renewal-type equation has been used in many earlier works (see [52] and references therein). In the limit $t \to \infty$, one gets

$$G_{0,\phi}(\boldsymbol{x}, t|\boldsymbol{x}_0) \xrightarrow{t\to\infty} \omega \tilde{G}_0(\boldsymbol{x}, \omega|\boldsymbol{x}_0), \quad (34)$$

in agreement with Eq. (24).

Other general expressions are also simplified for the Poissonian resetting. For instance, Eq. (26) reads

$$\mathcal{L}_{q,p}\{\rho_\omega(\ell, t|\boldsymbol{x}_0)\} = \tilde{S}_{q,\omega}(p|\boldsymbol{x}_0) = \frac{\tilde{S}_q(p+\omega|\boldsymbol{x}_0)}{1-\omega\tilde{S}_q(p+\omega|\boldsymbol{x}_0)}, \quad (35)$$

from which the probability density follows as

$$\tilde{H}_{q,\omega}(p|\boldsymbol{x}_0) = \frac{(p+\omega)\tilde{H}_q(p+\omega|\boldsymbol{x}_0)}{p+\omega\tilde{H}_q(p+\omega|\boldsymbol{x}_0)}. \quad (36)$$

This relation was reported by Reuveni and used to show that the relative standard deviation of the FPT is equal to 1 under optimal resetting [38] (see also [61]; a similar relation for the generating function was given in [35]; see a more general discussion in Sec. 3.1 of the review [52]). In particular, setting $p = 0$ in Eq. (35) yields the known expression for the mean FRT:

$$\mathbb{E}\{\mathcal{T}_\omega\} = \frac{\tilde{S}_q(\omega|\boldsymbol{x}_0)}{1-\omega\tilde{S}_q(\omega|\boldsymbol{x}_0)} = \frac{1-\tilde{H}_q(\omega|\boldsymbol{x}_0)}{\omega\tilde{H}_q(\omega|\boldsymbol{x}_0)}. \quad (37)$$

Expressing $\tilde{S}_q(p+\omega|\boldsymbol{x}_0)$ in terms of $\tilde{S}_{q,\omega}(p|\boldsymbol{x}_0)$ from Eq. (35) and then substituting it into Eq. (30) gives

$$\tilde{G}_{q,\omega}(\boldsymbol{x}, p|\boldsymbol{x}_0) = (1+\omega\tilde{S}_{q,\omega}(p|\boldsymbol{x}_0))\tilde{G}_q(\boldsymbol{x}, p+\omega|\boldsymbol{x}_0), \quad (38)$$

from which the double inverse Laplace transform with respect to p and q yields

$$P_\omega(\boldsymbol{x}, \ell, t|\boldsymbol{x}_0) = e^{-\omega t} P(\boldsymbol{x}, \ell, t|\boldsymbol{x}_0) + \int_0^t dt' \omega e^{-\omega(t-t')} \times \int_0^\ell d\ell' P(\boldsymbol{x}, \ell-\ell', t-t'|\boldsymbol{x}_0)\, \rho_\omega(\ell', t'|\boldsymbol{x}_0). \quad (39)$$

This is a typical renewal-type representation, in which the first term represents the contribution without resetting, while the second term accounts for resettings; in this term, the time interval from 0 to t is split by time t' of the *last* resetting before t, which occurs with the probability density $\omega e^{-\omega(t-t')}$. During the period from 0 to t', resettings erase information on the position so that $\rho_\omega(\ell', t'|\boldsymbol{x}_0)$ determines the boundary local time ℓ' acquired up to t'. In turn, as the position is reset to $\boldsymbol{x}_0$ at t', the diffusive dynamics from t' to t is described by $P(\boldsymbol{x}, \ell-\ell', t-t'|\boldsymbol{x}_0)$. The relation (39), which was also derived in [61], expresses the full propagator under Poissonian resetting in terms of $P(\boldsymbol{x}, \ell, t|\boldsymbol{x}_0)$ (without resetting) and the probability density $\rho_\omega(\ell, t|\boldsymbol{x}_0)$ with resetting. However, its explicit form is deceptive because $\rho_\omega(\ell, t|\boldsymbol{x}_0)$ still has to be determined via the double inverse Laplace transform of Eq. (35).

C. Boundary local time resetting

Now we turn to another resetting scenario, which was not studied earlier and consists in resetting the boundary local time ℓ_t, while keeping the position $\boldsymbol{X}_t$ unchanged. Such a resetting does not affect the dynamics of the particle; in particular, if the target is inert ($q = 0$), the related propagator $G_0(\boldsymbol{x}, t|\boldsymbol{x}_0)$ remains unchanged by construction. However, resetting of the boundary local time may affect the reaction mechanism on a reactive target. We aim, therefore, to analyze how such a resetting modifies the full propagator $P(\boldsymbol{x}, \ell, t|\boldsymbol{x}_0)$, the propagator $G_q(\boldsymbol{x}, t|\boldsymbol{x}_0)$, and the probability density $\rho(\ell, t|\boldsymbol{x}_0)$ of the boundary local time. We also discuss the (unsolved) challenges in computing the probability density $U(\ell, t|\boldsymbol{x}_0)$ of the first-crossing time.

1. Full propagator

Similarly to Eq. (17), one can write a renewal-type relation

$$P_\phi(\boldsymbol{x}, \ell, t|\boldsymbol{x}_0) = \Phi(t)P(\boldsymbol{x}, \ell, t|\boldsymbol{x}_0) + \int_0^t dt_1 \phi(t_1) \int_\Omega \int_0^\infty d\boldsymbol{x}_1 d\ell_1 P(x_1, \ell_1, t_1|\boldsymbol{x}_0)\, \Phi(t-t_1) P(\boldsymbol{x}, \ell, t-t_1|\boldsymbol{x}_1) + \cdots. \quad (40)$$

In contrast to the previous computation in Sec. II B, convolutions over boundary local times are replaced by integrals over their intermediate values. Using Eq. (11) with $q = 0$ to evaluate these integrals and performing the Laplace transform with respect to time t, we get

$$\tilde{P}_\phi(\boldsymbol{x}, \ell, p|\boldsymbol{x}_0) = \mathcal{L}_p\{\Phi(t)P(\boldsymbol{x}, \ell, t|\boldsymbol{x}_0)\} + \int_\Omega d\boldsymbol{x}_1 \mathcal{L}_p\{\phi(t) \times G_0(\boldsymbol{x}_1, t|\boldsymbol{x}_0)\}\mathcal{L}_p\{\Phi(t)P(\boldsymbol{x}, \ell, t|\boldsymbol{x}_1)\} + \cdots. \quad (41)$$

To proceed, one needs to evaluate the integrals over intermediate positions $\boldsymbol{x}_k \in \Omega$. For this purpose, we use the spectral decomposition (14) of the propagator $G_0(\boldsymbol{x}, t|\boldsymbol{x}_0)$. For instance, one has

$$\mathcal{L}_p\{\phi(t)G_0(\boldsymbol{x}, t|\boldsymbol{x}_0)\} = \sum_{k=0}^\infty u_k^{(0)}(\boldsymbol{x})\big[u_k^{(0)}(\boldsymbol{x}_0)\big]^* \tilde{\phi}\big(p + D\lambda_k^{(0)}\big). \quad (42)$$

The orthonormality of eigenfunctions $u_k^{(0)}(\boldsymbol{x})$ allows one to compute the integral of two such functions:

$$\begin{aligned}\int_\Omega d\boldsymbol{x}_1\, \mathcal{L}_p\{\phi(t)G_0(\boldsymbol{x}_1,t|\boldsymbol{x}_0)\}\, \mathcal{L}_p\{\phi(t)G_0(\boldsymbol{x},t|\boldsymbol{x}_1)\}&\\ = \sum_{k_1,k_2=0}^{\infty}\int_\Omega d\boldsymbol{x}_1\, \big(u_{k_1}^{(0)}(\boldsymbol{x}_1)\big[u_{k_1}^{(0)}(\boldsymbol{x}_0)\big]^*\tilde{\phi}\big(p+D\lambda_{k_1}^{(0)}\big)\big)&\\ \times\big(u_{k_2}^{(0)}(\boldsymbol{x})\big[u_{k_2}^{(0)}(\boldsymbol{x}_1)\big]^*\tilde{\phi}\big(p+D\lambda_{k_2}^{(0)}\big)\big)&\\ = \sum_{k=0}^{\infty} u_k^{(0)}(\boldsymbol{x})\big[u_k^{(0)}(\boldsymbol{x}_0)\big]^*\big[\tilde{\phi}\big(p+D\lambda_k^{(0)}\big)\big]^2.&\end{aligned}$$

More generally, the integral of over $n-1$ intermediate points $\boldsymbol{x}_1,\boldsymbol{x}_2,\ldots,\boldsymbol{x}_{n-1}$ yields the nth power of $\tilde{\phi}(p+D\lambda_k^{(0)})$. Using this property, we can sum the infinite number of terms in Eq. (41) to get

$$\begin{aligned}\tilde{P}_\phi(\boldsymbol{x},\ell,p|\boldsymbol{x}_0) = \int_\Omega d\boldsymbol{x}'\mathcal{L}_p\{\Phi(t)P(\boldsymbol{x},\ell,t|\boldsymbol{x}')\}&\\ \times\sum_{k=0}^{\infty}\frac{u_k^{(0)}(\boldsymbol{x}')\big[u_k^{(0)}(\boldsymbol{x}_0)\big]^*}{1-\tilde{\phi}\big(p+D\lambda_k^{(0)}\big)}.&\end{aligned}\tag{43}$$

An inverse Laplace transform with respect to p yields a formal solution for the full propagator $P_\phi(\boldsymbol{x},\ell,t|\boldsymbol{x}_0)$ under resetting of the boundary local time:

$$\begin{aligned}P_\phi(\boldsymbol{x},\ell,t|\boldsymbol{x}_0) = \int_\Omega d\boldsymbol{x}'\int_0^t dt'\,\xi(t')\,G_0(\boldsymbol{x}',t'|\boldsymbol{x}_0)&\\ \times\Phi(t-t')\,P(\boldsymbol{x},\ell,t-t'|\boldsymbol{x}'),&\end{aligned}\tag{44}$$

where

$$\xi(t) = \mathcal{L}_p^{-1}\left\{\frac{1}{1-\tilde{\phi}(p)}\right\}(t),\tag{45}$$

and we used again the spectral decomposition (14) of the propagator $G_0(\boldsymbol{x},t|\boldsymbol{x}_0)$.

It is instructive to look at the long-time behavior of the full propagator. As the position of the particle is not affected by resetting, it should reach the uniform distribution, as in the no-resetting case. In addition, random resettings of the boundary local time render this quantity stationary at long times as well. As a consequence, one can expect that the full propagator reaches a well-defined steady-state limit. This is indeed the case. To show it, let us examine Eq. (43) in the limit $p\to 0$, which corresponds to the long-time behavior. It is known that the principal eigenvalue $\lambda_0^{(0)}$ of the Laplace operator with Neumann boundary condition ($q=0$) is zero. In addition, the corresponding eigenfunction is constant: $u_0^{(0)} = |\Omega|^{-1/2}$. As a consequence, the sum in Eq. (43) behaves as $1/(p|\Omega|\mathbb{E}\{\delta\}) + O(1)$ as $p\to 0$, where we used $\tilde{\phi}(p)\approx 1-p\mathbb{E}\{\delta\}+O(p^2)$, under the assumption that the mean $\mathbb{E}\{\delta\}$ is finite. One sees that the right-hand side of Eq. (43) has a pole at $p=0$ that yields the constant term in the long-time limit:

$$P_\phi(\boldsymbol{x},\ell,t|\boldsymbol{x}_0)\xrightarrow{t\to\infty}P_\phi^{\rm st}(\boldsymbol{x},\ell) = \int_0^\infty\frac{dt\,\Phi(t)}{\mathbb{E}\{\delta\}}P(\boldsymbol{x},\ell,t|\circ),\tag{46}$$

where

$$P(\boldsymbol{x},\ell,t|\circ) = \frac{1}{|\Omega|}\int_\Omega d\boldsymbol{x}'\,P(\boldsymbol{x},\ell,t|\boldsymbol{x}')\tag{47}$$

can be interpreted as the full propagator averaged over the starting point uniformly distributed in Ω (here $\circ$ highlights that the starting point is uniformly distributed; we keep using this notation for other quantities). Expectedly, the steady-state distribution $P_\phi^{\rm st}(\boldsymbol{x},\ell)$ does not depend on the starting point $\boldsymbol{x}_0$.

Let us have a closer look at the steady-state limit $P_\phi^{\rm st}(\boldsymbol{x},\ell)$. On the one hand, its integral over ℓ yields the expected uniform distribution of the position:

$$\int_0^\infty d\ell\,P_\phi^{\rm st}(\boldsymbol{x},\ell) = \frac{1}{\mathbb{E}\{\delta\}}\int_0^\infty dt\,\Phi(t)G_0(\boldsymbol{x},t|\circ) = \frac{1}{|\Omega|},\tag{48}$$

where we used that $G_0(\boldsymbol{x},t|\circ) = 1/|\Omega|$ for any time t (if the initial distribution was uniform, it remains uniform for any t since the target is inert). On the other hand, the joint steady-state probability density $P_\phi^{\rm st}(\boldsymbol{x},\ell)$ is not factored, revealing correlations between $\boldsymbol{X}_t$ and ℓ_t. The steady-state probability density of the boundary local time reads

$$\rho_\phi^{\rm st}(\ell) = \int_\Omega d\boldsymbol{x}\,P_\phi^{\rm st}(\boldsymbol{x},\ell) = \frac{1}{\mathbb{E}\{\delta\}}\int_0^\infty dt\,\Phi(t)\rho(\ell,t|\circ),\tag{49}$$

where

$$\rho(\ell,t|\circ) = \frac{1}{|\Omega|}\int_\Omega d\boldsymbol{x}_0\,\rho(\ell,t|\boldsymbol{x}_0).\tag{50}$$

The expression (43) can be further simplified if the starting point $\boldsymbol{x}_0$ is not fixed but uniformly distributed in Ω. The orthogonality of eigenfunctions $u_k^{(0)}$ with $k>0$ to $u_0^{(0)} = |\Omega|^{-1/2}$ implies that the integral over $\boldsymbol{x}_0$ cancels all terms in the sum except $k=0$. After simplifications, we get

$$\begin{aligned}\tilde{P}_\phi(\boldsymbol{x},\ell,p|\circ) &= \frac{1}{|\Omega|}\int_\Omega d\boldsymbol{x}_0\,\tilde{P}_\phi(\boldsymbol{x},\ell,p|\boldsymbol{x}_0)\\ &= \frac{\mathcal{L}_p\{\Phi(t)P(\boldsymbol{x},\ell,t|\circ)\}}{1-\tilde{\phi}(p)}.\end{aligned}\tag{51}$$

For the Poissonian resetting, one has $\tilde{\phi}(p) = \omega/(\omega+p)$, which allows one to simplify Eq. (43) as

$$\begin{aligned}\tilde{P}_\omega(\boldsymbol{x},\ell,p|\boldsymbol{x}_0) = \tilde{P}(\boldsymbol{x},\ell,p+\omega|\boldsymbol{x}_0) + \omega\int_\Omega d\boldsymbol{x}'\,\tilde{G}_0(\boldsymbol{x}',p|\boldsymbol{x}_0)&\\ \times\tilde{P}(\boldsymbol{x},\ell,p+\omega|\boldsymbol{x}'),&\end{aligned}\tag{52}$$

which reads in the time domain as

$$\begin{aligned}P_\omega(\boldsymbol{x},\ell,t|\boldsymbol{x}_0) = e^{-\omega t}P(\boldsymbol{x},\ell,t|\boldsymbol{x}_0) + \int_0^t dt'\omega e^{-\omega(t-t')}&\\ \times\int_\Omega d\boldsymbol{x}'\,G_0(\boldsymbol{x}',t'|\boldsymbol{x}_0)\,P(\boldsymbol{x},\ell,t-t'|\boldsymbol{x}').&\end{aligned}\tag{53}$$

This relation has a simple probabilistic interpretation in terms of the last resetting time, in analogy to the discussion after Eq. (39). It could also be directly deduced from Eq. (44).

If the starting point $\boldsymbol{x}_0$ is distributed uniformly, the volume average of Eq. (52) yields

$$\tilde{P}_\omega(\boldsymbol{x}, \ell, p|\circ) = \tilde{P}(\boldsymbol{x}, \ell, p+\omega|\circ)\left(1+\frac{\omega}{p}\right), \tag{54}$$

where we used that

$$\int_\Omega d\boldsymbol{x}_0 \tilde{G}_0(\boldsymbol{x}', p|\boldsymbol{x}_0) = \int_\Omega d\boldsymbol{x}_0 \tilde{G}_0(\boldsymbol{x}_0, p|\boldsymbol{x}') = \frac{1}{p} \tag{55}$$

due to the normalization of the propagator $G_0(\boldsymbol{x}_0, t|\boldsymbol{x}')$ and its symmetry with respect to the exchange of the starting and arrival points. In the time domain, Eq. (54) reads

$$P_\omega(\boldsymbol{x}, \ell, t|\circ) = e^{-\omega t} P(\boldsymbol{x}, \ell, t|\circ) + \int_0^t dt' \omega e^{-\omega t'} P(\boldsymbol{x}, \ell, t'|\circ). \tag{56}$$

In the long-time limit, one retrieves

$$P_\omega(\boldsymbol{x}, \ell, t|\circ) \xrightarrow{t\to\infty} P_\omega^{\rm st}(\boldsymbol{x}, \ell) = \omega \tilde{P}(\boldsymbol{x}, \ell, \omega|\circ), \tag{57}$$

in agreement with the general relation (46).

The full propagator in Eq. (43) determines the probability density $\rho_\phi(\ell, t|\boldsymbol{x}_0)$ of the boundary local time under resetting. In the case of Poissonian resetting, the integral of Eq. (52) over $\boldsymbol{x} \in \Omega$ gives

$$\tilde{\rho}_\omega(\ell, p|\boldsymbol{x}_0) = \tilde{\rho}(\ell, p+\omega|\boldsymbol{x}_0) + \omega \int_\Omega d\boldsymbol{x}' \, \tilde{G}_0(\boldsymbol{x}', p|\boldsymbol{x}_0) \times \tilde{\rho}(\ell, p+\omega|\boldsymbol{x}'). \tag{58}$$

If the starting point $\boldsymbol{x}_0$ is distributed uniformly in Ω, the average over $\boldsymbol{x}_0$ yields

$$\tilde{\rho}_\omega(\ell, p|\circ) = \tilde{\rho}(\ell, p+\omega|\circ)\left(1+\frac{\omega}{p}\right), \tag{59}$$

which becomes in the time domain

$$\rho_\omega(\ell, t|\circ) = e^{-\omega t} \rho(\ell, t|\circ) + \int_0^t dt' \, \omega e^{-\omega t'} \, \rho(\ell, t'|\circ), \tag{60}$$

in analogy with Eq. (56).

In the long-time limit, one retrieves

$$\rho_\omega(\ell, t|\circ) \xrightarrow{t\to\infty} \rho_\omega^{\rm st}(\ell) = \omega \tilde{\rho}(\ell, \omega|\circ), \tag{61}$$

in agreement with the general relation (49).

To complete this discussion, let us check whether the symmetry of the full propagator under the exchange of the starting and arrival points $\boldsymbol{x}_0$ and $\boldsymbol{x}$ is preserved or not. This was the case for the full propagator $P(\boldsymbol{x}, \ell, t|\boldsymbol{x}_0)$ without resetting; see Eq. (16). As resettings of the boundary local time do not affect the position $\boldsymbol{X}_t$, one might think that the symmetry is preserved here. However, an inspection of Eq. (43) reveals that this symmetry is in general broken for the full propagator $P_\phi(\boldsymbol{x}, \ell, t|\boldsymbol{x}_0)$ under resetting. What does break the symmetry? Even though the random trajectory $\boldsymbol{X}_t$ of the diffusing particle remains unaffected, resettings modify the boundary local time ℓ_t and thus affect *correlations* between $\boldsymbol{X}_t$ and ℓ_t, which are captured by the full propagator $P_\phi(\boldsymbol{x}, \ell, t|\boldsymbol{x}_0)$. To better illustrate this point, let us consider the situation with a single resetting at time t_1. The path from $\boldsymbol{x}_0$ to $\boldsymbol{x}$ is then split into two parts: the path from $\boldsymbol{x}_0$ to an intermediate position $\boldsymbol{X}_{t_1} = \boldsymbol{x}_1$, which is sampled without any constraint on the intermediate boundary local time ℓ_1 (ranging from 0 to ∞), and the path from $\boldsymbol{x}_1$ to $\boldsymbol{x}$ with the constraint on ℓ_t to be ℓ. The reversed path from $\boldsymbol{x}$ to $\boldsymbol{x}_0$ (after the exchange of the starting and arrival points) is also split into two similar parts: from $\boldsymbol{x}$ to $\boldsymbol{x}_1$ without constraint on the boundary local time, and from $\boldsymbol{x}_1$ to $\boldsymbol{x}_0$ with such a constraint. The presence of a constraint changes the statistics and thus breaks the symmetry. This is particularly clear from Eq. (52) for the Poissonian resetting: the part without constraint is sampled with $\tilde{G}_0(\boldsymbol{x}_1, p|\boldsymbol{x}_0)$, whereas the part with constraint is sampled with $\tilde{P}(\boldsymbol{x}, \ell, p+\omega|\boldsymbol{x}_1)$.

2. Conventional propagator

In contrast to Eq. (11) in the no-resetting case, the full propagator $P_\phi(\boldsymbol{x}, \ell, t|\boldsymbol{x}_0)$ under resetting, given by Eq. (43), does not allow one to access the propagator $G_{q,\phi}(\boldsymbol{x}, t|\boldsymbol{x}_0)$. In fact, one can no longer use the fundamental relation (11) because the monotonous growth of the boundary local time is broken by resettings. Even if the survival probability of the particle is still determined as $\mathbb{E}\{e^{-\mu T_t}\}$ by the total residence time T_t of the particle in the vicinity of the target, the latter is not given by $a\ell_t/D$ but should include the boundary local times acquired upon all prior resettings. If there were k resettings up to time t at times $t_1, \ldots, t_k$, then

$$T_t = \frac{a}{D} L_t, \quad L_t = \ell_{t_1} + \cdots + \ell_{t_k} + \ell_t, \tag{62}$$

where ℓ_{t_j} is the boundary local time acquired between two successive resettings at t_{j-1} and t_j, while ℓ_t is the boundary local time acquired between t_k (the last resetting) and t. As a consequence, the integral over all intermediate states should be done with the survival probability

$$e^{-qL_t} = e^{-q\ell_{t_1}} \cdots e^{-q\ell_{t_k}} \, e^{-q\ell_t}, \tag{63}$$

i.e., each resetting is "penalized" by the corresponding factor $e^{-q\ell_{t_j}}$:

$$\begin{aligned} G_{q,\phi}(\boldsymbol{x}, t|\boldsymbol{x}_0) &= \Phi(t) G_q(\boldsymbol{x}, t|\boldsymbol{x}_0) + \int_0^t dt_1 \phi(t_1) \int_\Omega d\boldsymbol{x}_1 \\ &\quad \times \int_0^\infty d\ell_1 e^{-q\ell_1} P(\boldsymbol{x}_1, \ell_1, t_1|\boldsymbol{x}_0) \Phi(t-t_1) \\ &\quad \times \int_0^\infty d\ell e^{-q\ell} P(\boldsymbol{x}, \ell, t-t_1|\boldsymbol{x}_1) + \cdots . \end{aligned} \tag{64}$$

The integrals over boundary local times eliminate these variables and allow one to replace full propagators by the conventional propagators:

$$\begin{aligned} &G_{q,\phi}(\boldsymbol{x}, t|\boldsymbol{x}_0) \\ &\quad = \Phi(t) G_q(\boldsymbol{x}, t|\boldsymbol{x}_0) + \int_0^t dt_1 \phi(t_1) \\ &\qquad \times \int_\Omega d\boldsymbol{x}_1 G_q(\boldsymbol{x}_1, t_1|\boldsymbol{x}_0) \Phi(t-t_1) G_q(\boldsymbol{x}, t-t_1|\boldsymbol{x}_1) + \cdots . \end{aligned}$$

In turn, the Laplace transform with respect to t transforms time convolutions into products. Finally, the integrals over intermediate positions $\boldsymbol{x}_1, \boldsymbol{x}_2$, etc. can be calculated by using the spectral decomposition (14) of the propagators and the orthonormality of Laplacian eigenfunctions. In analogy to

Eq. (43), we get

$$\tilde{G}_{q,\phi}(\boldsymbol{x}, p|\boldsymbol{x}_0) = \int_\Omega d\boldsymbol{x}' \mathcal{L}_p\{\Phi(t) G_q(\boldsymbol{x}', t|\boldsymbol{x}_0)\} \times \sum_{k=0}^{\infty} \frac{u_k^{(q)}(\boldsymbol{x})\big[u_k^{(q)}(\boldsymbol{x}')\big]^*}{1-\tilde{\phi}\big(p+D\lambda_k^{(q)}\big)}.$$

However, the main difference with Eq. (43) is that the factor $\mathcal{L}_p\{\Phi(t)G_q(\boldsymbol{x}', t|\boldsymbol{x}_0)\}$ itself admits the same spectral decomposition that allows one to compute the integral over $\boldsymbol{x}'$:

$$\tilde{G}_{q,\phi}(\boldsymbol{x}, p|\boldsymbol{x}_0) = \sum_{k=0}^{\infty} u_k^{(q)}(\boldsymbol{x})\big[u_k^{(q)}(\boldsymbol{x}_0)\big]^* \frac{\tilde{\Phi}\big(p+D\lambda_k^{(q)}\big)}{1-\tilde{\phi}\big(p+D\lambda_k^{(q)}\big)}.$$

Finally, as $\Phi(t)$ is the integral of $\phi(t)$, one has $\tilde{\Phi}(p) = [1-\tilde{\phi}(p)]/p$ so that the last factor is simply $1/(p+D\lambda_k^{(q)})$. Inverting this Laplace transform with respect to p, one gets

$$G_{q,\phi}(\boldsymbol{x}, t|\boldsymbol{x}_0) = G_q(\boldsymbol{x}, t|\boldsymbol{x}_0) \tag{65}$$

for any resetting. In essence, the above formal derivation reflects the fact that the product of exponential penalizing factors in Eq. (63) can be reduced to a single factor e^{-qL_t}, where L_t represents the total boundary local time as if there was no resetting.

We stress that the identity (65) is a consequence of the *chosen* mechanism of surface reactions. In general, however, the constant reactivity can be replaced by other surface reaction mechanisms [53], which is mathematically equivalent to replacing the exponential law for the random threshold $\hat{\ell}$ by another law: $\mathbb{P}\{\hat{\ell} > \ell\} = \Psi(\ell)$. The overall "penalizing" factor Eq. (63) is now replaced by

$$\Psi(\ell_{t_1})\cdots\Psi(\ell_{t_k})\,\Psi(\ell_t), \tag{66}$$

which is in general not equal to $\Psi(L_t)$. As a consequence, splitting the total boundary local time L_t into "pieces" $\ell_{t_1}, \ldots, \ell_{t_k}, \ell_t$ by resettings changes the penalizing factor from $\Psi(L_t)$ to the product in Eq. (66) and thus modifies the generalized propagator $G_{\Psi,\phi}(\boldsymbol{x}, t|\boldsymbol{x}_0)$ under resetting so that

$$G_{\Psi,\phi}(\boldsymbol{x}, t|\boldsymbol{x}_0) \neq G_\Psi(\boldsymbol{x}, t|\boldsymbol{x}_0) \tag{67}$$

in general. It is worth noting that the generalized propagator $G_\Psi(\boldsymbol{x}, t|\boldsymbol{x}_0)$, given by Eq. (12), does not satisfy the Robin boundary condition (13b) and thus does not possess a spectral expansion on common Laplacian eigenfunctions, like Eq. (14) for the conventional propagator $G_q(\boldsymbol{x}, t|\boldsymbol{x}_0)$. In particular, one cannot evaluate the integrals over the intermediate positions $\boldsymbol{x}_k$ in the same way as we did for the derivation of Eq. (43). Finding appropriate tools to compute the generalized propagator $G_{\Psi,\phi}(\boldsymbol{x}, t|\boldsymbol{x}_0)$ under resetting presents an interesting perspective for future research.

3. Probability density of the first-crossing time

Moreover, even for the constant reactivity, one can imagine other settings, for which the boundary local time resetting would affect the conventional propagator. For instance, resetting can model a renewal of the reactive state of the target or of the particle, therefore erasing the former history of their interactions. For instance, in the context of a resource depletion model introduced in [60], the particle receives a unit of resources at each encounter with the target, while a threshold ℓ characterizes the amount of initially available resources. In this setting, the first-crossing time $\mathcal{T}_\ell$ defined by Eq. (10) is the first-depletion time, at which the resources on the target are exhausted. In turn, the boundary local time resetting can be considered as a replenishment of resources to the initial level ℓ. The depletion dynamics is therefore characterized by the probability density $U_\phi(\ell, t|\boldsymbol{x}_0)$ of the first-crossing time under resetting. In contrast to the no-resetting case (Sec. II A), the density $U_\phi(\ell, t|\boldsymbol{x}_0)$ does not follow from the full propagator and related quantities. For instance, $\rho_\phi(\ell, t|\boldsymbol{x}_0)$ determines the probability $\mathbb{P}\{\ell_t < \ell\}$ that the boundary local time ℓ_t *at time* t does not exceed the level ℓ; however, as ℓ_t is not monotonously increasing due to resettings, this probability says nothing about the values of $\ell_{t'}$ at earlier times t'. In other words, the processes ℓ_t and $\ell_t^{\max} = \max_{0<t'<t}\{\ell_{t'}\}$ are not identical anymore. It is therefore the probability law for $\ell_t^{\max}$ that determines the first-crossing time $\mathcal{T}_\ell$. In analogy with Eq. (40), one can write the renewal-type relation for the joint probability density of $\boldsymbol{X}_t$ and $\ell_t^{\max}$ as

$$P_\phi^{\max}(\boldsymbol{x}, \ell, t|\boldsymbol{x}_0) = \Phi(t)P(\boldsymbol{x}, \ell, t|\boldsymbol{x}_0) + \int_0^t dt_1 \phi(t_1) \int_\Omega \int_0^\ell d\boldsymbol{x}_1 d\ell_1 P(x_1, \ell_1, t_1|\boldsymbol{x}_0)\,\Phi(t-t_1)P(\boldsymbol{x}, \ell, t-t_1|\boldsymbol{x}_1) + \cdots. \tag{68}$$

Once this infinite series is computed, the distribution of the first-crossing time under resetting can be determined via

$$\mathbb{P}\{T_\ell > t\} = \mathbb{P}\big\{\ell_t^{\max} < \ell\big\} = \int_0^\ell d\ell' \int_\Omega d\boldsymbol{x}\, P_\phi^{\max}(\boldsymbol{x}, \ell', t|\boldsymbol{x}_0). \tag{69}$$

The "only" difference with Eq. (40) is that the integrals over ℓ_k in Eq. (68) have an upper limit ℓ instead of ∞, to ensure that intermediate boundary local times ℓ_k do not exceed the threshold ℓ. However, this change does not allow one to replace full propagators by $G_0(\boldsymbol{x}, t|\boldsymbol{x}_0)$, while the spectral expansions of the resulting integrated full propagators are more sophisticated and do not allow us to simply evaluate integrals over intermediate positions $\boldsymbol{x}_k$. This challenging problem remains unsolved, even for the Poissonian resetting.

III. DIFFUSION ON AN INTERVAL

To illustrate our general results, we consider diffusion on an interval $(0, b)$ of length b with partially reactive end

points (i.e., $\Gamma = \{0, b\}$). For this basic example, most quantities of interest can be found explicitly and easily drawn. Note that this one-dimensional setting is equivalent to three-dimensional diffusion between parallel planes separated by distance b. Similar explicit computations should be feasible for other common models, such as, e.g., a disk, a cylinder, a sphere, or a spherical target surrounded by a concentric spherical boundary (see [54,55]). We stress that former works on resetting dealt with unbounded domains so that "finite-size effects" have been ignored.

The conventional propagator $G_q(x, t|x_0)$ is well known, and was reported in different textbooks (see, e.g., [90,91]). In particular, the Laplace transform of the propagator is given by (see, e.g., [54])

$$\tilde{G}_q(x, p|x_0) = \frac{1}{\alpha V D} \times \begin{cases} v_q(x) v_q(b - x_0) & (0 \leqslant x \leqslant x_0), \\ v_q(x_0) v_q(b - x) & (x_0 \leqslant x \leqslant b), \end{cases} \tag{70}$$

where $\alpha = \sqrt{p/D}$ and

$$v_q(x) = q \sinh(\alpha x) + \alpha \cosh(\alpha x), \tag{71}$$

$$V = (\alpha^2 + q^2) \sinh(\alpha b) + 2\alpha q \cosh(\alpha b). \tag{72}$$

The Laplace-transformed survival probability then reads

$$\tilde{S}_q(p|x_0) = \frac{1}{pV}(\alpha^2 \sinh(\alpha b) + q^2(\sinh(\alpha b) - \sinh(\alpha(b - x_0)) - \sinh(\alpha x_0)) + \alpha q(2\cosh(\alpha b) - \cosh(\alpha(b - x_0)) - \cosh(\alpha x_0))). \tag{73}$$

In the limit $q \to \infty$, one gets

$$\tilde{S}_\infty(p|x_0) = \frac{1}{p}\left(1 - \frac{\sinh(\alpha x_0) + \sinh(\alpha(b - x_0))}{\sinh(\alpha b)}\right). \tag{74}$$

The Laplace-transformed full propagator was found in [54]. When $0 \leqslant x \leqslant x_0 \leqslant b$, one has [92]

$$\tilde{P}(x, \ell, p|x_0) = \tilde{G}_\infty(x, p|x_0)\delta(\ell) + \frac{e^{-C\ell}}{D \sinh^2(\alpha b)}\{(\sinh(\alpha(b - x_0)) \sinh(\alpha(b - x)) + \sinh(\alpha x_0) \sinh(\alpha x)) \cosh(E\ell) + (\sinh(\alpha(b - x_0)) \sinh(\alpha x) + \sinh(\alpha x_0) \sinh(\alpha(b - x))) \sinh(E\ell)\}, \tag{75}$$

with $C = \alpha \coth(\alpha b)$ and $E = \frac{\alpha}{\sinh(\alpha b)}$ (if $0 \leqslant x_0 \leqslant x \leqslant b$, one has to exchange x_0 and x). The probability density of ℓ_t is given by

$$\tilde{\rho}(\ell, p|x_0) = \tilde{S}_\infty(p|x_0)\delta(\ell) + \frac{e^{-(C-E)\ell}}{D} \times \frac{\cosh(\alpha b) - 1}{\alpha \sinh(\alpha b)} \frac{\sinh(\alpha x_0) + \sinh(\alpha(b - x_0))}{\sinh(\alpha b)}. \tag{76}$$

We emphasize that the behavior of this density is drastically different from the classical Lévy's result for diffusion on the half-line,

$$\rho(\ell, t|x_0) = \mathrm{erf}\left(\frac{x_0}{\sqrt{4Dt}}\right)\delta(\ell) + \frac{\exp\left(-\frac{(x_0+\ell)^2}{4Dt}\right)}{\sqrt{\pi D t}}, \tag{77}$$

where $\mathrm{erf}(z)$ is the error function (see the discussion in [93]). Note that Eq. (77) can be easily deduced by taking the limit $b \to \infty$ in Eq. (76) and computing the inverse Laplace transform. The full propagator on the half-line is also known explicitly; see [55]. The volume-average of Eq. (76) yields

$$\tilde{\rho}(\ell, p|\circ) = \frac{1}{b}\int_0^b dx_0\, \tilde{\rho}(\ell, p|x_0) = \tilde{S}_\infty(p|\circ)\delta(\ell) + \frac{e^{-(C-E)\ell}}{bD} \frac{2[\cosh(\alpha b) - 1]^2}{\alpha^2 \sinh^2(\alpha b)}, \tag{78}$$

where

$$\tilde{S}_\infty(p|\circ) = \frac{1}{p}\left(1 - 2\frac{\cosh(\alpha b) - 1}{\alpha b \sinh(\alpha b)}\right). \tag{79}$$

Note that the symmetry (16) of the full propagator implies that

$$\tilde{P}(x, \ell, p|\circ) = \frac{1}{b}\int_0^b dx_0\, \underbrace{\tilde{P}(x, \ell, p|x_0)}_{=\tilde{P}(x_0, \ell, p|x)} = \frac{1}{b}\tilde{\rho}(\ell, p|x), \tag{80}$$

i.e., it is given by Eq. (76). Using these expressions, one can construct different quantities under resetting. For illustrative purposes, we focus on the Poissonian resetting $\Phi(t) = e^{-\omega t}$.

We set $b = 1$ and $D = 1$ to fix units of length and time. In particular, the diffusion timescale can be estimated as $t_{\mathrm{diff}} = b^2/(D\pi^2) \approx 0.1$, where π^2/b^2 is the smallest eigenvalue $\lambda_0^{(\infty)}$ for perfectly reactive end points. Moreover, in the case of inert end points, one also has $\lambda_1^{(0)} = \pi^2/b^2$ that controls the asymptotic approach to the uniform distribution. In other words, t_{diff} is a typical time needed for the diffusing particle to explore the confining domain. This timescale distinguishes low ($\omega t_{\mathrm{diff}} \ll 1$), moderate ($\omega t_{\mathrm{diff}} \sim 1$), and high ($\omega t_{\mathrm{diff}} \gg 1$) resetting rates. Note also that we usually consider three values of the reactivity parameter: $q = 0$ (inert target), $q = 1$ (moderately reactive target), and $q = \infty$ (perfectly reactive target).

Figure 1 shows a random trajectory X_t of the particle and its boundary local time ℓ_t for two types of resetting concerning either the position, or the boundary local time.

A. Position resetting

We start by looking at the effect of position resetting on the propagator $G_{q,\omega}(x, t|x_0)$, which can be obtained from the inverse Laplace transform of Eq. (30). Even though both $\tilde{G}_q(x, p|x_0)$ and $\tilde{S}_q(p|x_0)$ are known explicitly, we compute the inverse Laplace transform numerically by using the Talbot algorithm.

Figure 2 illustrates the effect of the resetting rate ω onto the propagator $G_{q,\omega}(x, t|x_0)$ at $t = 0.1$ (i.e., at the diffusion

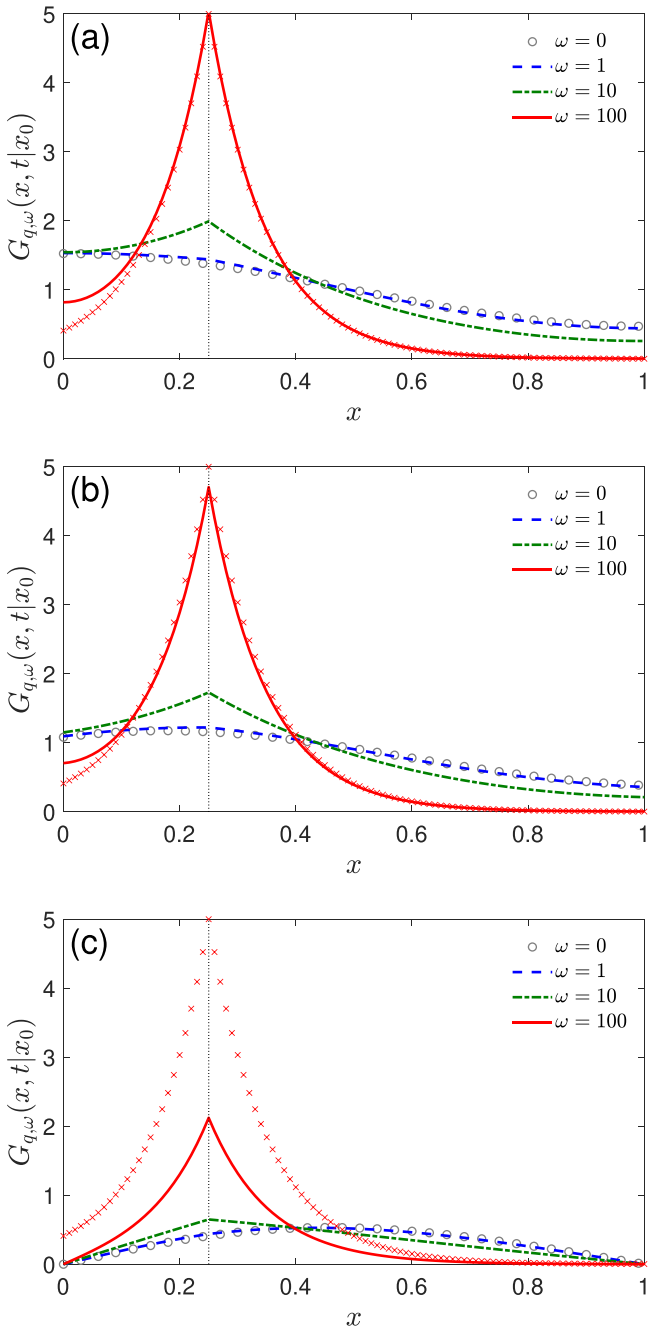

FIG. 2. The propagator $G_{q,\omega}(x,t|x_0)$ under Poissonian resetting of the position at the rate ω for diffusion on the unit interval ($b = 1$), with $x_0 = 0.25$, $t = 0.1$, $D = 1$, four values of ω (see the legend), and $q = 0$ (a), $q = 1$ (b), and $q = \infty$ (c). Note that $\omega = 0$ corresponds to the propagator $G_q(x,t|x_0)$ without resetting. Vertical dotted line indicates the position x_0. Crosses present the steady-state density in Eq. (82) at $\omega = 100$ for the whole line without any target.

time $t_{\rm diff}$) for three values of the reactivity parameter q. When $\omega = 1$, resettings are too rare and have little effect on the propagator (we recall that $\omega = 0$ corresponds to the propagator without resetting). At $\omega = 10$, there are only few resettings during time $t = 0.1$ but their effect is clearly seen. It is further amplified at $\omega = 100$. When the target is inert ($q = 0$), resettings prevent the approach of $G_{0,\omega}(x,t|x_0)$ to the uniform distribution 1, increasing the likelihood of finding the particle near its starting point x_0 [panel (a)]. In this case, the propagator $G_{0,\omega}(x,t|x_0)$ approaches its steady-state limit $G^{\rm st}_\omega(x|x_0) = \omega\tilde{G}_0(x,\omega|x_0)$ given by Eq. (70). In the limit $b \to \infty$, this expression tends to the steady-state density on the positive half-line with a reflecting end point at the origin:

$$G^{\rm st}_\omega(x|x_0) = \frac{\alpha}{2} e^{-\alpha|x-x_0|}(1 + e^{-2\alpha \min\{x,x_0\}}), \tag{81}$$

with $\alpha = \sqrt{\omega/D}$. Moreover, if the reflecting end point is moved to $-\infty$, the last factor approaches 1, and one retrieves the seminal result for diffusion on the whole line with resetting [25]:

$$G^{\rm st}_\omega(x|x_0) = \frac{\alpha}{2} e^{-\alpha|x-x_0|}. \tag{82}$$

A distinct cusplike feature of this function is clearly visible in Fig. 2(a) for $\omega = 10$ and 100. Moreover, it accurately describes the behavior of the propagator $G_{0,\omega}(x,t|x_0)$ near x_0 at the high resetting rate.

For reactive targets ($q > 0$), the steady-state distribution is zero in both cases with or without resetting. In turn, frequent resettings delay the reaction event and thus prolong the survival of the particle. A cusplike behavior at high resetting rates ω is also present in panels (b) and (c) of Fig. 2.

This is also consistent with an increase of the mean first-reaction time $\mathbb{E}\{\mathcal{T}_\omega\}$ as $\omega \to \infty$. In fact, the substitution of Eq. (73) into Eq. (37) yields an exact fully explicit expression for $\mathbb{E}\{\mathcal{T}_\omega\}$. In the limit $\omega \to 0$, one retrieves the classical result

$$\mathbb{E}\{\mathcal{T}_0\} = \frac{x_0(b-x_0)}{2D} + \frac{b}{2qD} \tag{83}$$

without resetting. In turn, if $b\sqrt{\omega/D} \gg 1$, one has

$$\tilde{S}_q(p|x_0) \approx \frac{1}{p}\left(1 - \frac{q}{q+\alpha} e^{-\alpha x_0}\right) \tag{84}$$

for $0 < x_0 < b/2$, which implies a very simple approximation to the mean FRT:

$$\mathbb{E}\{\mathcal{T}_\omega\} \approx \frac{(1+\sqrt{\omega/D}/q)e^{x_0\sqrt{\omega/D}} - 1}{\omega}. \tag{85}$$

This approximation becomes exact for diffusion on the half-line with a partially reactive origin (i.e., in the limit $b \to \infty$), so that one retrieves the mean first-passage time reported in [25] for $q = \infty$ (perfect target) and in [34] for $q < \infty$. Note that an additional factor 2 in front of $\sqrt{\omega/D}/q$ appears in Eq. (35) from [34] due to the fact that the target was treated as "two-sided," i.e., the particle diffused on the whole line and could cross the target, accessing it from the left and from the right; in turn, we consider that the target is impenetrable and can be accessed only from the positive semiaxis.

In the limit $\omega \to \infty$, there is an exponentially fast growth of the mean FRT. However, if x_0 is small enough, this growth is preceded by a decay that ensures a minimum of the mean FRT [25]. This behavior is very sensitive to the starting point x_0. Even though the confining domain is bounded here, resetting to a point near the target can considerably speed up the search process and the consequent reaction. Figure 3 illustrates the behavior of the mean FRT for both perfectly and partially reactive targets. An approach to a finite limit (83) as

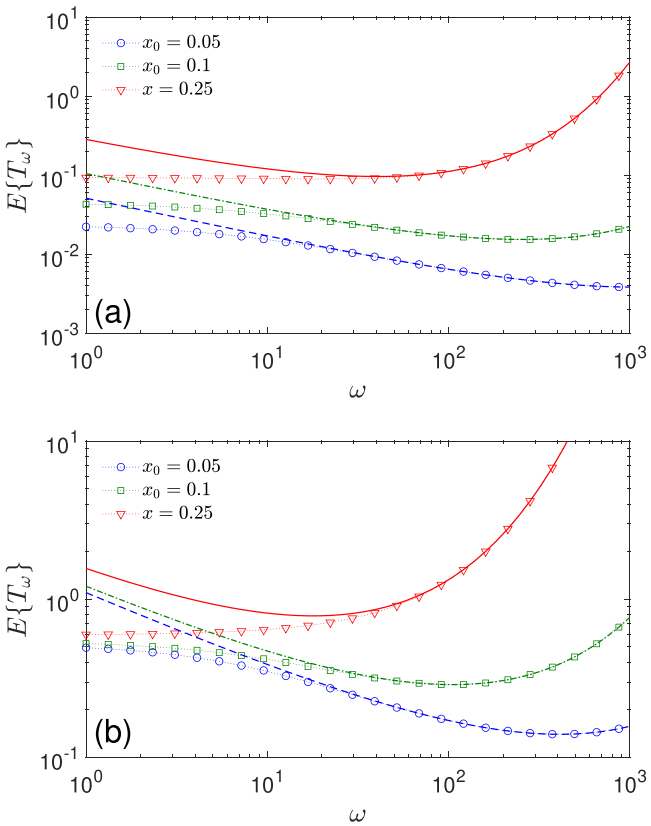

FIG. 3. The mean first-reaction time $\mathbb{E}\{\mathcal{T}_\omega\}$ under Poissonian resetting of the position at rate ω for diffusion on the unit interval ($b = 1$), with $D = 1$, three values of x_0 (see the legend), $q = \infty$ (a), and $q = 1$ (b). Symbols show the exact result (37) with $\tilde{S}_q(p|x_0)$ from Eq. (73), while lines illustrate the approximate relation (85).

$\omega \to 0$ is the finite-size effect due to the boundedness of the confining domain, which was not reported in earlier works. In particular, if the starting point is not close to the target (e.g., $x_0 = 0.25$), the minimum of the mean FRT occurs at $\omega = 0$, i.e., without resetting. One sees that finding the optimality range of diffusive search in bounded domains under resetting can actually be more difficult than in unbounded domains.

In Appendix A, we also computed the Laplace-transformed probability density $\tilde{U}_\omega(\ell, p|x_0)$ that determines the first-crossing time under Poissonian resetting of the position. A numerical inversion of the Laplace transform in Eq. (A6) yields this density in the time domain. Figures 4(a) and 4(b) illustrate the effect of the Poissonian resetting onto $U_\omega(\ell, t|x_0)$. When the starting point x_0 is relatively far from the target [$x_0 = 0.25$, panel (a)], weak ($\omega = 1$) and moderate ($\omega = 10$) resettings have almost no impact on the probability density [it remains close to $U_0(\ell, t|x_0)$ without resetting]. However, at frequent resettings ($\omega = 100$), the particle cannot stay long enough near the target, which slows down the growth of the boundary local time ℓ_t and thus increases the first-crossing time. The effect of resetting is opposite when the starting point is located on the target [$x_0 = 0$, panel (b)]. Here, the particle is reset on the target, which speeds up the growth of the boundary local time and thus decreases the first-crossing time. When the starting point is close to the target, one can

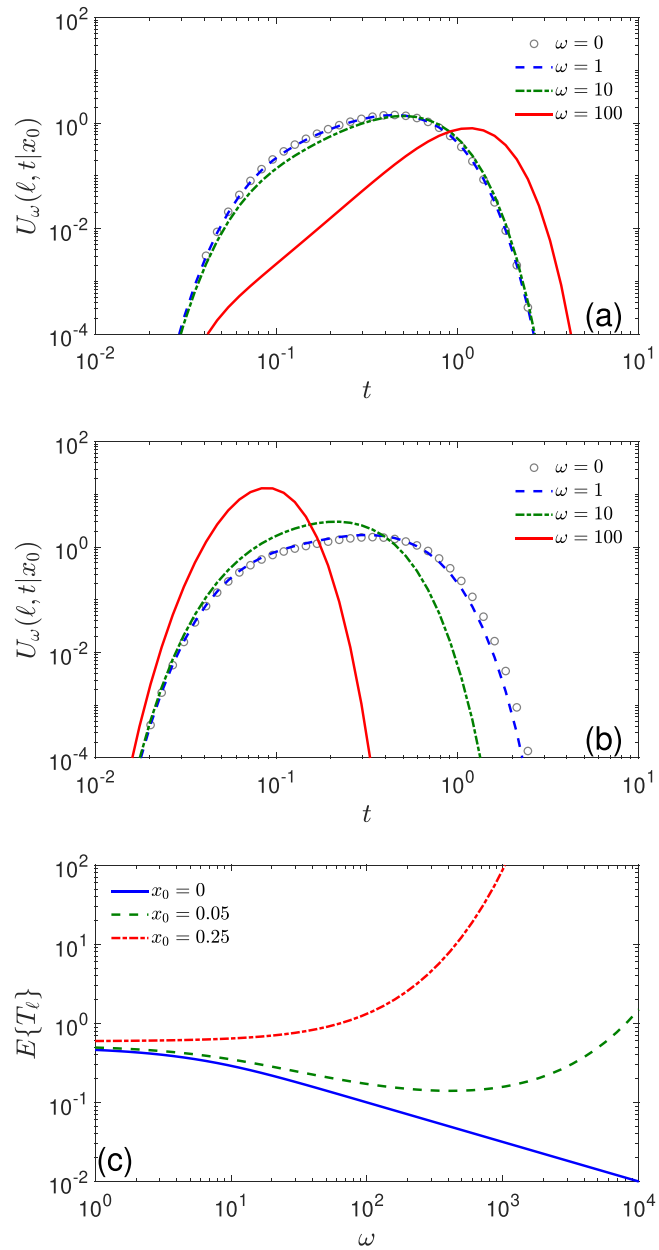

FIG. 4. (a), (b) The probability density $U_\omega(\ell, t|x_0)$ of the first-crossing time $\mathcal{T}_\ell$ under Poissonian resetting of the position at the rate ω for diffusion on the unit interval ($b = 1$), with $D = 1$, $\ell = 1$, four values of ω (see the legend), $x_0 = 0.25$ (a), and $x_0 = 0$ (b). The density was obtained by the numerical inversion of the Laplace transform in Eq. (A6) via the Talbot algorithm. (c) The mean first-crossing time $\mathbb{E}\{\mathcal{T}_\ell\}$ under Poissonian resetting as a function of the rate ω, for $\ell = 1$ and three values of x_0 (see the legend). $\mathbb{E}\{\mathcal{T}_\ell\}$ was obtained as the derivative of Eq. (A6) with respect to p, evaluated at $p = 0$.

therefore expect that resetting can optimize the first-crossing time $\mathcal{T}_\ell$, in particular its mean value. Figure 4(c) illustrates this statement. This behavior will be studied elsewhere.

B. Boundary local time resetting

Now we turn to the analysis of the Poissonian resetting of the boundary local time. The distribution of the boundary local time without resetting was studied in [54,93–95]

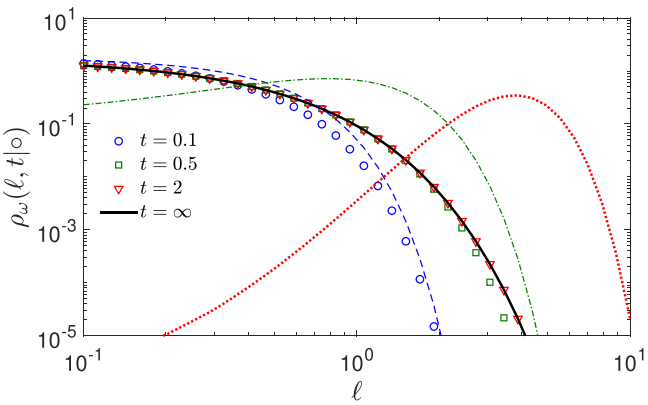

FIG. 5. The regular part of the probability density $\rho_\omega(\ell, t|\circ)$ of the boundary local time ℓ_t under Poissonian resetting, with $D = 1$, $b = 1$, and several times t (see the legend). Thin lines show the case without resetting ($\omega = 0$), while symbols present the case with moderate resetting ($\omega = 10$). A thick black line indicates the steady-state probability density $\rho_\omega^{\rm st}(\ell)$ from Eq. (61).

(see also references therein). We recall that the probability density $\rho(\ell, t|\boldsymbol{x}_0)$ has two contributions: a singular part $S_\infty(t|\boldsymbol{x}_0)\delta(\ell)$ from the trajectories that never reached the target up to time t (and thus $\ell_t = 0$), and a regular part from the remaining trajectories. As the first contribution is trivial, we focus on the regular part. To avoid secondary effects of the starting point location, we consider the volume-averaged probability density $\rho_\omega(\ell, t|\circ)$ that exhibits similar features. This quantity is obtained by inversion of the Laplace transform in Eq. (59) via the Talbot algorithm, with $\tilde{\rho}(\ell, p|\circ)$ given by Eq. (78).

Figure 5 illustrates the behavior of $\rho_\omega(\ell, t|\circ)$. When there is no resetting (thin lines), the maximum of the probability density $\rho(\ell, t|\circ)$ is progressively shifted to larger ℓ. This is consistent with the fact that, in a bounded domain, the mean boundary local time grows linearly with t at long times (see, e.g., [93]). In turn, resetting drastically changes this nonstationary character (see Sec. II C) so that $\rho_\omega(\ell, t|\circ)$ approaches a steady-state limit $\rho_\omega^{\rm st}(\ell)$ given in Eq. (61). This is clearly seen for $t = 0.5$ (squares) and $t = 2$ (triangles), for which $\rho_\omega(\ell, t|\circ)$ almost coincides with $\rho_\omega^{\rm st}(\ell)$ (thick black line). In turn, at moderate time $t = 0.1$, the probability density $\rho_\omega(\ell, t|\circ)$ is still close to $\rho(\ell, t|\circ)$, i.e., the effect of resetting is weak at this timescale.

Figure 6 shows the regular part of the volume-averaged full propagator $P_\omega(x, \ell, t|\circ)$ evaluated at $t = 1$. In the case without resetting ($\omega = 0$), this quantity was studied in [54]. Figure 6(a) shows the expected behavior of the full propagator without resetting; in particular, one observes a maximum with respect to the boundary local time ℓ, which is progressively shifted to larger ℓ as t grows (in other words, the "wave" shown at $t = 1$ moves in the direction of increasing ℓ). As the dependence of $P(x, \ell, t|\circ)$ on the position x is less visible here, we show it more explicitly in Fig. 7(a), where $P(x, \ell, t|\circ)$ is plotted against x for multiple values of ℓ ranging from 0 to 4. As we are unlikely to get too small values of ℓ at $t = 1$, $P(x, \ell, t|\circ)$ at small ℓ (blue curves) has a small amplitude and exhibits a maximum at the middle of the interval. In fact, it is easier for the particle found at the middle to have

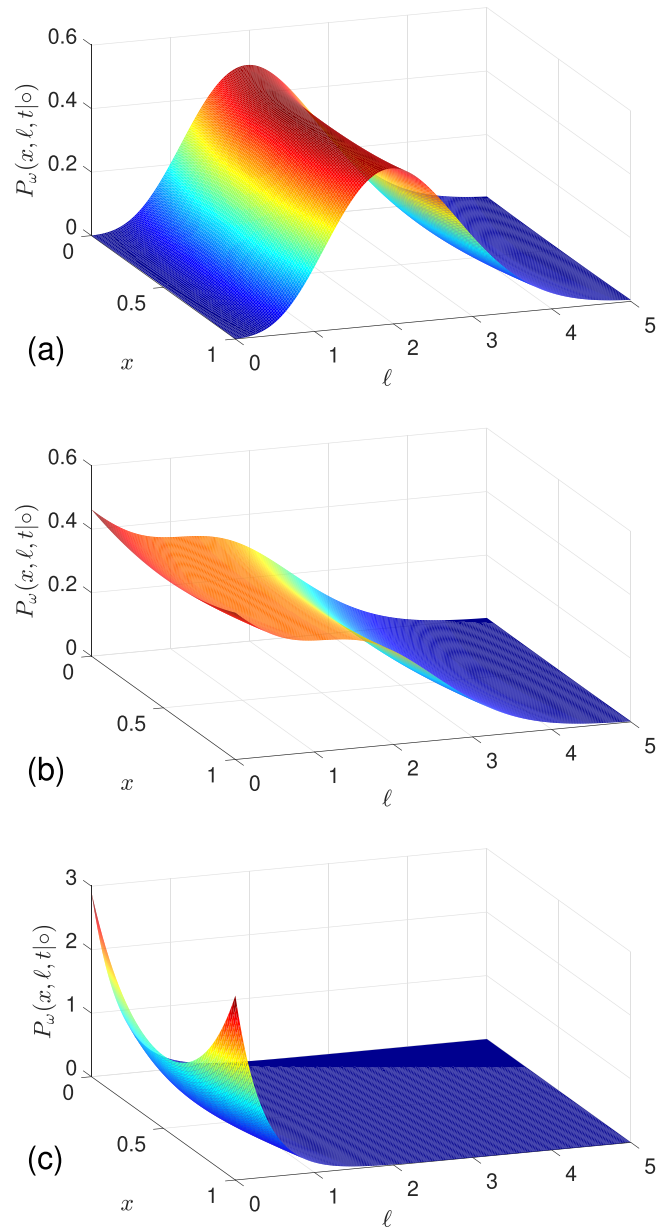

FIG. 6. The regular part of the volume-averaged full propagator $P_\omega(x, \ell, t|\circ)$ under Poissonian resetting of the boundary local time at rate ω for diffusion on the unit interval ($b = 1$), with $D = 1$, $b = 1$, $t = 1$, $\omega = 0$ (a), $\omega = 1$ (b), and $\omega = 10$ (c). $P_\omega(x, \ell, t|\circ)$ was obtained from Eq. (54) by numerical inversion of the Laplace transform.

smaller values of ℓ by encountering the target less frequently. Similarly, we are unlikely to get too large values of ℓ so that $P(x, \ell, t|\circ)$ at large ℓ (red curves) has a small amplitude and exhibits a minimum at the middle of the interval. Here, it is easier for the particle located near the end points to encounter the target more frequently and thus to acquire larger ℓ. This behavior illustrates correlations between X_t and ℓ_t.

In the presence of resetting, the behavior of the volume-averaged full propagator $P_\omega(x, \ell, t|\circ)$ is qualitatively different [Figs. 6(b) and 6(c)]. At large t, this propagator reaches the steady-state distribution $P_\omega^{\rm st}(x, \ell)$, which is given by Eq. (57)

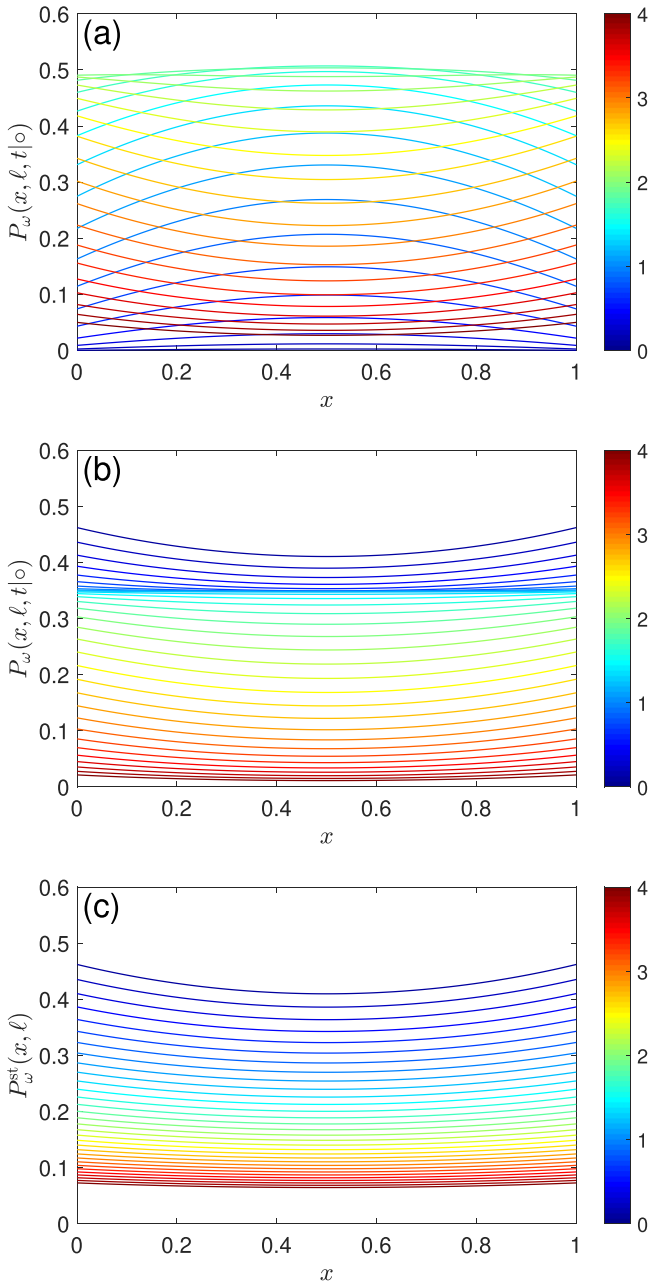

FIG. 7. The regular part of the volume-averaged full propagator $P_\omega(x,\ell,t|\circ)$ under Poissonian resetting of the boundary local time at rate ω for diffusion on the unit interval ($b=1$). It is plotted as a function x for multiple values of ℓ, with $D=1$. Three panels correspond to $t=1$, $\omega=0$ (a); $t=1$, $\omega=1$ (b); and $t=\infty$, $\omega=1$ (c). 33 colored curves correspond to 33 equally spaced values of ℓ ranging from 0 (dark blue) to 4 (dark red).

and reads for diffusion on the interval as

$$P^{\rm st}_\omega(x,\ell)=\frac{\omega}{b}\Bigg(\tilde{S}_\infty(\omega|x)\delta(\ell)+\frac{\cosh(\alpha b)-1}{\alpha D\sinh^2(\alpha b)}\times e^{-\alpha\tanh(\alpha b/2)\ell}\left(\sinh(\alpha x)+\sinh\left(\alpha(b-x)\right)\right)\Bigg), \tag{86}$$

with $\alpha=\sqrt{\omega/D}$. The first (singular) term accounts for the trajectories that do not reach the target after the last resetting and thus have $\ell_t=0$. In turn, we focus on the second (regular) term corresponding to $\ell>0$. Here, the dependences on ℓ and x are factored out so that $P^{\rm st}_\omega(x,\ell)$ always exhibits a minimum at $x=b/2$, whose amplitude is progressively attenuated as ℓ increases. This behavior is also illustrated in panels (b) and (c) of Fig. 7.

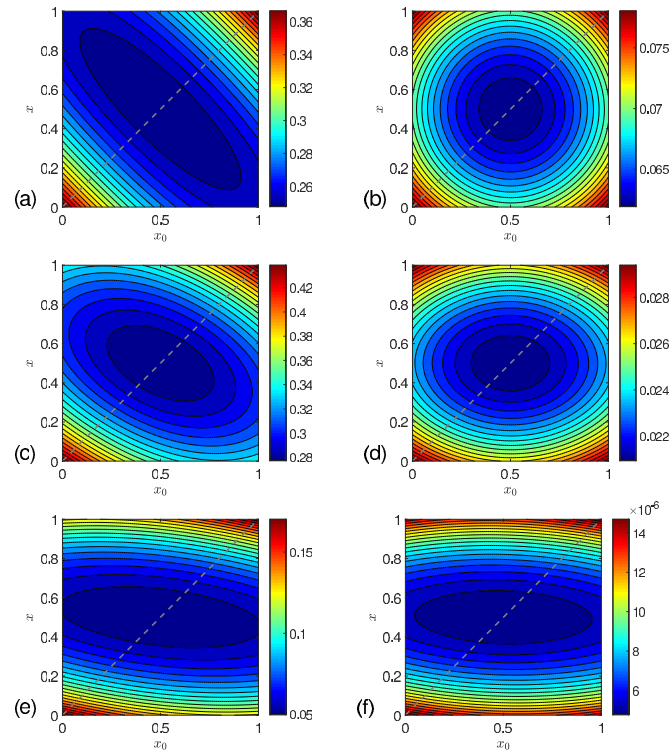

FIG. 8. Colored contour plots of the Laplace-transformed full propagator $\tilde{P}_\omega(x,\ell,p|x_0)$ under Poissonian resetting of the boundary local time at rate ω for diffusion on the unit interval ($b=1$), with $D=1$, $p=1$, $\ell=1$ (left column), and $\ell=4$ (right column). Panels correspond to $\omega=0$ (a), (b); $\omega=1$ (c), (d); and $\omega=10$ (e), (f).

Finally, we illustrate the asymmetry of the full propagator with respect to the exchange of points $\boldsymbol{x}_0$ and $\boldsymbol{x}$ (see Sec. II C). Even though the integral in Eq. (52) can be calculated exactly, the resulting formulas are too cumbersome so that we perform a numerical integration. We also stick to the Laplace domain without performing its numerical inversion. Figure 8 presents a contour plot of the Laplace-transformed full propagator $\tilde{P}_\omega(x,\ell,p|x_0)$ at fixed values of ℓ and p, and several values of the resetting rate ω. At $\omega=0$ [panels (a) and (b)], this plot is symmetric with respect to the diagonal (shown by a dashed gray line). In turn, when $\omega>0$ [panels (c)–(f)], an asymmetry emerges and is getting more and more visible as ω increases. In particular, the function $\tilde{P}_\omega(x,\ell,p|x_0)$ at $\omega=10$ almost does not depend on x_0.

IV. CONCLUSION

In this paper, we investigated the effect of stochastic resetting onto diffusion-controlled reactions within the encounter-based approach. On the one hand, this approach disentangles the diffusive dynamics from surface reactions, yielding a deeper insight into the search process and allowing

one to implement more sophisticated surface reaction mechanisms [53]. On the other hand, it offers richer opportunities for implementing the stochastic resetting: while former works were focused on resetting the position of the particle, one can now investigate the effect of the boundary local time resetting as well. We followed these two scenarios and derived two formal representations (21) and (44) of the full propagator $P_\phi(\boldsymbol{x}, \ell, t|\boldsymbol{x}_0)$ under arbitrary resetting. These results allow one to access many other quantities under resetting, such as the conventional propagator $G_{q,\phi}(\boldsymbol{x}, t|\boldsymbol{x}_0)$, the survival probability $S_{q,\phi}(t|\boldsymbol{x}_0)$, the probability density $H_{q,\phi}(t|\boldsymbol{x}_0)$ of the first-reaction time $\mathcal{T}_\phi$ and its mean value $\mathbb{E}\{\mathcal{T}_\phi\}$, the probability density $\rho_\phi(\ell, t|\boldsymbol{x}_0)$ of the boundary local time ℓ_t, and the probability density $U_\phi(\ell, t|\boldsymbol{x}_0)$ of the first-crossing time $\mathcal{T}_\ell$. In the case of position resetting, our general formalism allowed us to deduce some earlier obtained expressions. In particular, we retrieved the general expression for the mean first-reaction time and its asymptotic behavior for one-dimensional diffusion. In turn, the scenario of the boundary local time resetting has been introduced here so that all the results that we obtained in Sec. II C were not reported earlier. In particular, we showed that the full propagator approaches a steady-state distribution and studied its behavior. We also observed the asymmetry of the full propagator with respect to the exchange of the starting and arrival points, which originates from subtle correlations between the position and the boundary local time. Quite counterintuitively, we found that the conventional propagator is not affected by any resetting of the boundary local time. We showed, however, that this is a specific feature of the constant reactivity and the related exponential distribution in the stopping condition. This property does not necessarily hold for other surface reaction mechanisms. The impact of stochastic resetting in this more general setting remains to be uncovered.

While we managed to compute most quantities of interest, at least in the Laplace domain, the problem of finding the probability density $U_\phi(\ell, t|\boldsymbol{x}_0)$ of the first-crossing time under resetting of the boundary local time remains unsolved. As described in Sec. II C, such resetting events destroy the nondecreasing character of the boundary local time ℓ_t so that ℓ_t is no longer equal to its maximum, $\ell_t^{\max} = \max_{0<t'<t}\{\ell_{t'}\}$. As a consequence, the knowledge of ℓ_t is not enough for describing the probability law of $\ell_t^{\max}$ or, equivalently, the first-crossing time. Even though one can still write a renewal-type equation (68) for the joint probability density of $\boldsymbol{X}_t$ and $\ell_t^{\max}$, we could not find a way to compute the integrals over intermediate positions $\boldsymbol{x}_k$ and thus to sum up all the contributions. This is a challenging open problem.

Quite naturally, one can go beyond the above two types of resetting. If both the position and the boundary local time are reset simultaneously, the full propagator gets a particularly simple form:

$$\tilde{P}_\phi(\boldsymbol{x}, \ell, p|\boldsymbol{x}_0) = \frac{\mathcal{L}_p\{\Phi(t)P(\boldsymbol{x}, \ell, t|\boldsymbol{x}_0)\}}{1-\tilde{\phi}(p)}. \tag{87}$$

In the case of the Poissonian resetting, one has

$$\tilde{P}_\omega(\boldsymbol{x}, \ell, p|\boldsymbol{x}_0) = \left(1+\frac{\omega}{p}\right)\tilde{P}(\boldsymbol{x}, \ell, p+\omega|\boldsymbol{x}_0), \tag{88}$$

which reads in the time domain as

$$P_\omega(\boldsymbol{x}, \ell, t|\boldsymbol{x}_0) = e^{-\omega t}P(\boldsymbol{x}, \ell, t|\boldsymbol{x}_0) + \int_0^t dt'\, \omega e^{-\omega t'}\, P(\boldsymbol{x}, \ell, t'|\boldsymbol{x}_0). \tag{89}$$

This relation was also derived in [61], where the case of simultaneous resettings of the position and the boundary local time was studied in more detail; in particular, the generalized propagator $\tilde{G}_{\Psi,\omega}(\boldsymbol{x}, p|\boldsymbol{x}_0)$ under Poissonian resetting but arbitrary surface reaction mechanism $\Psi(\ell)$ was obtained. There exist, however, more general forms of asynchronized resettings of $\boldsymbol{X}_t$ and ℓ_t, which may considerably affect the full propagator and the related quantities. Further explorations in this direction present an interesting perspective.

As our study was realized independently and in parallel to the work by Bressloff [61], it is instructive to highlight several distinctions between them. (i) The analysis in [61] was focused on the Poissonian resetting, which can be implemented by modifying the partial differential equations for the full propagator and related quantities. This method presents some advantages; in particular, Bressloff derived the governing equations for the propagator $G_{\Psi,\omega}(\boldsymbol{x}, t|\boldsymbol{x}_0)$ with a general surface reaction mechanism. However, its extension to other resetting laws is difficult. In turn, we employed the renewal scheme, which is applicable to any resetting law. (ii) Bressloff considered two resetting scenarios: resetting of the position alone and simultaneous resetting of both $\boldsymbol{X}_t$ and ℓ_t; while we also looked at the first scenario, our main focus was on resetting of the boundary local time alone, which is technically more difficult. (iii) The analysis of [61] was formulated for diffusion outside a compact obstacle $\mathcal{U}$, i.e., for $\Omega = \mathbb{R}^d\backslash\mathcal{U}$, in contrast to our focus on bounded domains; even though many general results are valid in both settings, we often relied on spectral expansions, which are exclusively applicable in bounded domains, for which the Laplace operator has a discrete spectrum. (iv) Finally, Bressloff considered the exterior of a ball for illustrating his results, whereas we used a bounded domain (an interval). We conclude that these two works provide complementary insights onto the problem of diffusion-mediated surface phenomena with resetting.

Note added. At the submission of this paper, we discovered a recently published paper [61] that undertakes a similar study in the case of Poissonian resetting. Even though all our results were obtained independently, we systematically outline eventual overlaps with Ref. [61]; in addition, a comparison between two approaches is given in Sec. IV.

ACKNOWLEDGMENT

D.S.G. acknowledges the Alexander von Humboldt Foundation for support within a Bessel Prize award.

APPENDIX: COMPUTATION OF $U_\omega(\ell, t|\boldsymbol{x}_0)$

In this Appendix, we detail the computation of the Laplace-transformed probability density $\tilde{U}_\omega(\ell, p|x_0)$ of the first-crossing time under Poissonian resetting of the position

for diffusion on the interval. According to Eq. (73), we get

$$\tilde{H}_q(p|x_0) = q\frac{qS(x_0) + \alpha C(x_0)}{V}, \tag{A1}$$

where $S(x_0) = \sinh(\alpha(b - x_0)) + \sinh(\alpha x_0)$ and $C(x_0) = \cosh(\alpha(b - x_0)) + \cosh(\alpha x_0)$. We can then express

$$\tilde{H}_{q,\omega}(p|x_0) = \frac{(p+\omega)\tilde{H}_q(p+\omega|x_0)}{p + \omega\tilde{H}_q(p+\omega|x_0)} = \frac{q(p+\omega)[qS(x_0) + \alpha C(x_0)]}{aq^2 + bq + c}, \tag{A2}$$

where

$$a = p\sinh(\alpha b) + \omega S(x_0), \tag{A3a}$$

$$b = 2p\alpha\cosh(\alpha b) + \omega\alpha C(x_0), \tag{A3b}$$

$$c = p\alpha^2\sinh(\alpha b), \tag{A3c}$$

and we set $\alpha = \sqrt{(p+\omega)/D}$. Denoting by $q_\pm$ two roots of the quadratic polynomial in the denominator of Eq. (A2),

$$q_\pm = \frac{-b \pm \sqrt{b^2 - 4ac}}{2a}, \tag{A4}$$

one can decompose $\tilde{H}_{q,\omega}(p|x_0)/q$ into a sum of partial fractions

$$\frac{\tilde{H}_{q,\omega}(p|x_0)}{q} = \frac{(p+\omega)}{a(q_+ - q_-)}\left(\frac{q_+S(x_0) + \alpha C(x_0)}{q - q_+} - \frac{q_-S(x_0) + \alpha C(x_0)}{q - q_-}\right). \tag{A5}$$

Substituting this expression into Eq. (28), we compute explicitly the inverse Laplace transform with respect to q:

$$\tilde{U}_\omega(\ell, p|x_0) = \frac{p+\omega}{a(q_+ - q_-)}((q_+S(x_0) + \alpha C(x_0))e^{q_+\ell} - (q_-S(x_0) + \alpha C(x_0))e^{q_-\ell}). \tag{A6}$$

Since both roots $q_\pm$ are negative, this expression behaves correctly at large ℓ.

This is an exact fully explicit expression for the Laplace-transformed probability density of the first-crossing time under position resetting. Even though the inverse Laplace transform with respect to p is needed to get this quantity in the time domain, one can investigate the asymptotic behavior or compute the moments of the first-crossing time via the small-p expansion. For instance, one can check the correct normalization of the probability density: $\tilde{U}_\omega(\ell, 0|x_0) = 1$. In the limit $\omega \to 0$, one has $q_\pm = -\alpha(\cosh(\alpha b) \pm 1)/\sinh(\alpha b)$ that implies

$$\tilde{U}_0(\ell, p|x_0) = \frac{e^{-\ell\alpha\tanh(\alpha b/2)}}{\sinh(\alpha b)}(\sinh(\alpha(b - x_0)) + \sinh(\alpha x_0)) \tag{A7}$$

without resetting.

[1] S. Rice, *Diffusion-Limited Reactions* (Elsevier, Amsterdam, 1985).

[2] D. A. Lauffenburger and J. Linderman, *Receptors: Models for Binding, Trafficking, and Signaling* (Oxford University Press, Oxford, 1993).

[3] S. Redner, *A Guide to First Passage Processes* (Cambridge University Press, Cambridge, 2001).

[4] Z. Schuss, *Brownian Dynamics at Boundaries and Interfaces in Physics, Chemistry and Biology* (Springer, New York, 2013).

[5] *First-Passage Phenomena and Their Applications*, edited by R. Metzler, G. Oshanin, and S. Redner (World Scientific, Singapore, 2014).

[6] *Chemical Kinetics: Beyond the Textbook*, edited by K. Lindenberg, R. Metzler, and G. Oshanin (World Scientific, New Jersey, 2019).

[7] M. Smoluchowski, Versuch einer Mathematischen Theorie der Koagulations Kinetic Kolloider Lösungen, Z. Phys. Chem. **92U**, 129 (1918).

[8] H. C. Berg and E. M. Purcell, Physics of chemoreception, Biophys. J. **20**, 193 (1977).

[9] G. H. Weiss, Overview of theoretical models for reaction rates, J. Stat. Phys. **42**, 3 (1986).

[10] S. Condamin, O. Bénichou, V. Tejedor, R. Voituriez, and J. Klafter, First-passage time in complex scale-invariant media, Nature (London) **450**, 77 (2007).

[11] D. S. Grebenkov, NMR survey of reflected brownian motion, Rev. Mod. Phys. **79**, 1077 (2007).

[12] O. Bénichou and R. Voituriez, Narrow-Escape Time Problem: Time Needed for a Particle to Exit a Confining Domain through a Small Window, Phys. Rev. Lett. **100**, 168105 (2008).

[13] O. Bénichou, D. S. Grebenkov, P. Levitz, C. Loverdo, and R. Voituriez, Optimal Reaction Time for Surface-Mediated Diffusion, Phys. Rev. Lett. **105**, 150606 (2010).

[14] O. Bénichou, C. Chevalier, J. Klafter, B. Meyer, and R. Voituriez, Geometry-controlled kinetics, Nat. Chem. **2**, 472 (2010).

[15] O. Bénichou, C. Loverdo, M. Moreau, and R. Voituriez, Intermittent search strategies, Rev. Mod. Phys. **83**, 81 (2011).

[16] P. C. Bressloff and J. M. Newby, Stochastic models of intracellular transport, Rev. Mod. Phys. **85**, 135 (2013).

[17] A. J. Bray, S. N. Majumdar, and G. Schehr, Persistence and First-Passage Properties in Non-equilibrium Systems, Adv. Phys. **62**, 225 (2013).

[18] O. Bénichou and R. Voituriez, From first-passage times of random walks in confinement to geometry-controlled kinetics, Phys. Rep. **539**, 225 (2014).

[19] A. Godec and R. Metzler, First passage time distribution in heterogeneity controlled kinetics: going beyond the mean first passage time, Sci. Rep. **6**, 20349 (2016).

[20] A. Godec and R. Metzler, Universal Proximity Effect in Target Search Kinetics in the Few-Encounter Limit, Phys. Rev. X **6**, 041037 (2016).

[21] D. S. Grebenkov, Universal Formula for the Mean First Passage Time in Planar Domains, Phys. Rev. Lett. **117**, 260201 (2016).

[22] A. V. Chechkin, F. Seno, R. Metzler, and I. M. Sokolov, Brownian yet Non-Gaussian Diffusion: From Superstatistics to Subordination of Diffusing Diffusivities, Phys. Rev. X **7**, 021002 (2017).

[23] Y. Lanoiselée, N. Moutal, and D. S. Grebenkov, Diffusion-limited reactions in dynamic heterogeneous media, Nat. Commun. **9**, 4398 (2018).

[24] N. Levernier, M. Dolgushev, O. Bénichou, R. Voituriez, and T. Guérin, Survival probability of stochastic processes beyond persistence exponents, Nat. Commun. **10**, 2990 (2019).

[25] M. R. Evans and S. N. Majumdar, Diffusion with Stochastic Resetting, Phys. Rev. Lett. **106**, 160601 (2011).

[26] W. Feller, Diffusion processes in one dimension, Trans. Am. Math. Soc. **77**, 1 (1954).

[27] B. Sherman, The limiting distribution of brownian motion in a bounded region with instantaneous return, Ann. Math. Stat. **29**, 267 (1958).

[28] I. Grigorescu and M. Kang, Brownian motion on the figure eight, J. Theor. Prob. **15**, 817 (2002).

[29] Y. Leung, W. Li, and Rakesh, Spectral analysis of Brownian motion with jump boundary, Proc. Am. Math. Soc. **136**, 4427 (2008).

[30] I. Ben-Ari and R. G. Pinsky, Ergodic behavior of diffusions with random jumps from the boundary, Stoch. Proc. Appl. **119**, 864 (2009).

[31] B. De Bruyne, J. Randon-Furling, and S. Redner, Optimization in First-Passage Resetting, Phys. Rev. Lett. **125**, 050602 (2020).

[32] B. De Bruyne, J. Randon-Furling, and S. Redner, Optimization and growth in first-passage resetting, J. Stat. Mech. (2021) 013203.

[33] M. R. Evans and S. N. Majumdar, Diffusion with optimal resetting, J. Phys. A **44**, 435001 (2011).

[34] J. Whitehouse, M. R. Evans, and S. N. Majumdar, Effect of partial absorption on diffusion with resetting, Phys. Rev. E **87**, 022118 (2013).

[35] L. Kusmierz, S. N. Majumdar, S. Sabhapandit, and G. Schehr, First Order Transition for the Optimal Search Time of Lévy Flights with Resetting, Phys. Rev. Lett. **113**, 220602 (2014).

[36] V. Mendéz, A. Masó-Puigdellosas, T. Sandev, and D. Campos, Continuous time random walks under Markovian resetting, Phys. Rev. E **103**, 022103 (2021).

[37] A. Pal, A. Kundu, and M. R. Evans, Diffusion under time-dependent resetting, J. Phys. A **49**, 225001 (2016).

[38] S. Reuveni, Optimal Stochastic Restart Renders Fluctuations in First Passage Times Universal, Phys. Rev. Lett. **116**, 170601 (2016).

[39] S. Reuveni, M. Urbakh, and J. Klafter, Role of substrate unbinding in michaelis-menten enzymatic reactions, Proc. Natl. Acad. Sci. USA **111**, 4391 (2014).

[40] A. Pal and S. Reuveni, First Passage under Restart, Phys. Rev. Lett. **118**, 030603 (2017).

[41] A. V. Chechkin and I. M. Sokolov, Random Search with Resetting: A Unified Renewal Approach, Phys. Rev. Lett. **121**, 050601 (2018).

[42] M. R. Evans and S. N. Majumdar, Effects of refractory period on stochastic resetting, J. Phys. A **52**, 01LT01 (2019).

[43] A. S. Bodrova and I. M. Sokolov, Continuous-time random walks under power-law resetting, Phys. Rev. E **101**, 062117 (2020).

[44] A. Masó-Puigdellosas, D. Campos, and V. Mendéz, Transport properties and first-arrival statistics of random motion with stochastic reset times, Phys. Rev. E **99**, 012141 (2019).

[45] M. Dahlenburg, A. V. Chechkin, R. Schumer, and R. Metzler, Stochastic resetting by a random amplitude, Phys. Rev. E **103**, 052123 (2021).

[46] A. Pal, Diffusion in a potential landscape with stochastic resetting, Phys. Rev. E **91**, 012113 (2015).

[47] S. Ahmad, K. Rijal, and D. Das, First passage in the presence of stochastic resetting and a potential barrier, Phys. Rev. E **105**, 044134 (2022).

[48] J. M. Meylahn, S. Sabhapandit, and H. Touchette, Large deviations for Markov processes with resetting, Phys. Rev. E **92**, 062148 (2015).

[49] F. den Hollander, S. N. Majumdar, J. M. Meylahn, and H. Touchette, Properties of additive functionals of Brownian motion with resetting, J. Phys. A **52**, 175001 (2019).

[50] N. R. Smith and S. N. Majumdar, Condensation transition in large deviations of self-similar Gaussian processes with stochastic resetting, J. Stat. Mech. (2022) 053212.

[51] O. Tal-Friedman, A. Pal, A. Sekhon, S. Reuveni, and Y. Roichman, Experimental realization of diffusion with stochastic resetting, J. Phys. Chem. Lett. **11**, 7350 (2020).

[52] M. R. Evans, S. N. Majumdar, and G. Schehr, Stochastic resetting and applications, J. Phys. A **53**, 193001 (2020).

[53] D. S. Grebenkov, Paradigm Shift in Diffusion-Mediated Surface Phenomena, Phys. Rev. Lett. **125**, 078102 (2020).

[54] D. S. Grebenkov, Joint distribution of multiple boundary local times and related first-passage time problems, J. Stat. Mech. (2020) 103205.

[55] D. S. Grebenkov, Surface hopping propagator: An alternative approach to diffusion-influenced reactions, Phys. Rev. E **102**, 032125 (2020).

[56] D. S. Grebenkov, Statistics of boundary encounters by a particle diffusing outside a compact planar domain, J. Phys. A **54**, 015003 (2021).

[57] P. C. Bressloff, Narrow capture problem: An encounter-based approach to partially reactive targets, Phys. Rev. E **105**, 034141 (2022).

[58] D. S. Grebenkov, An encounter-based approach for restricted diffusion with a gradient drift, J. Phys. A **55**, 045203 (2022).

[59] P. C. Bressloff, Diffusion-mediated absorption by partially-reactive targets: Brownian functionals and generalized propagators, J. Phys. A **55**, 205001 (2022).

[60] D. S. Grebenkov, Depletion of resources by a population of diffusing species, Phys. Rev. E **105**, 054402 (2022).

[61] P. C. Bressloff, Diffusion-mediated surface reactions and stochastic resetting, J. Phys. A **55**, 275002 (2022).

[62] P. Lévy, *Processus Stochastiques et Mouvement Brownien* (Gauthier-Villard, Paris, 1965).

[63] K. Ito and H. P. McKean, *Diffusion Processes and Their Sample Paths* (Springer-Verlag, Berlin, 1965).

[64] M. Freidlin, *Functional Integration and Partial Differential Equations*, Annals of Mathematics Studies (Princeton University Press, Princeton, NJ, 1985).

[65] A. Comtet, J. Desbois, and S. N. Majumdar, The local time distribution of a particle diffusing on a graph, J. Phys. A **35**, L687 (2002).

[66] S. N. Majumdar and A. Comtet, Local and Occupation Time of a Particle Diffusing in a Random Medium, Phys. Rev. Lett. **89**, 060601 (2002).

[67] S. N. Majumdar, Brownian functionals in physics and computer science, Curr. Sci. **89**, 2076 (2005).

[68] A. Pal, R. Chatterjee, S. Reuveni, and A. Kundu, Local time of diffusion with stochastic resetting, J. Phys. A **52**, 264002 (2019).

[69] F. C. Collins and G. E. Kimball, Diffusion-controlled reaction rates, J. Coll. Sci. **4**, 425 (1949).

[70] H. Sano and M. Tachiya, Partially diffusion-controlled recombination, J. Chem. Phys. **71**, 1276 (1979).

[71] H. Sano and M. Tachiya, Theory of diffusion-controlled reactions on spherical surfaces and its application to reactions on micellar surfaces, J. Chem. Phys. **75**, 2870 (1981).

[72] D. Shoup and A. Szabo, Role of diffusion in ligand binding to macromolecules and cell-bound receptors, Biophys. J. **40**, 33 (1982).

[73] B. Sapoval, General Formulation of Laplacian Transfer Across Irregular Surfaces, Phys. Rev. Lett. **73**, 3314 (1994).

[74] M. Filoche and B. Sapoval, Can One Hear the Shape of an Electrode? II. Theoretical Study of the Laplacian Transfer, Eur. Phys. J. B **9**, 755 (1999).

[75] O. Bénichou, M. Moreau, and G. Oshanin, Kinetics of stochastically gated diffusion-limited reactions and geometry of random walk trajectories, Phys. Rev. E **61**, 3388 (2000).

[76] B. Sapoval, M. Filoche, and E. Weibel, Smaller is better—but not too small: A physical scale for the design of the mammalian pulmonary acinus, Proc. Natl. Acad. Sci. USA **99**, 10411 (2002).

[77] D. S. Grebenkov, M. Filoche, and B. Sapoval, Spectral properties of the brownian self-transport operator, Eur. Phys. J. B **36**, 221 (2003).

[78] D. S. Grebenkov, M. Filoche, B. Sapoval, and M. Felici, Diffusion-Reaction in Branched Structures: Theory and Application to the Lung Acinus, Phys. Rev. Lett. **94**, 050602 (2005).

[79] D. S. Grebenkov, M. Filoche, and B. Sapoval, Mathematical basis for a general theory of Laplacian transport towards irregular interfaces, Phys. Rev. E **73**, 021103 (2006).

[80] D. S. Grebenkov, Partially reflected Brownian motion: A stochastic approach to transport phenomena, in *Focus on Probability Theory*, edited by L. R. Velle (Nova Science,New York, 2006), pp. 135–169.

[81] S. D. Traytak and W. Price, Exact solution for anisotropic diffusion-controlled reactions with partially reflecting conditions, J. Chem. Phys. **127**, 184508 (2007).

[82] P. C. Bressloff, B. A. Earnshaw, and M. J. Ward, Diffusion of protein receptors on a cylindrical dendritic membrane with partially absorbing traps, SIAM J. Appl. Math. **68**, 1223 (2008).

[83] A. Singer, Z. Schuss, A. Osipov, and D. Holcman, Partially reflected diffusion, SIAM J. Appl. Math. **68**, 844 (2008).

[84] D. S. Grebenkov, Searching for partially reactive sites: Analytical results for spherical targets, J. Chem. Phys. **132**, 034104 (2010).

[85] D. S. Grebenkov, Subdiffusion in a bounded domain with a partially absorbing-reflecting boundary, Phys. Rev. E **81**, 021128 (2010).

[86] S. D. Lawley and J. P. Keener, A new derivation of robin boundary conditions through homogenization of a stochastically switching boundary, SIAM J. Appl. Dyn. Syst. **14**, 1845 (2015).

[87] D. S. Grebenkov, Analytical representations of the spread harmonic measure density, Phys. Rev. E **91**, 052108 (2015).

[88] A. Chaigneau and D. S. Grebenkov, First-passage times to anisotropic partially reactive targets, Phys. Rev. E **105**, 054146 (2022).

[89] S. M. Ross, *Introduction to Probability Models*, 11th ed. (Academic, Oxford, 2014).

[90] H. S. Carslaw and J. C. Jaeger, *Conduction of Heat in Solids*, 2nd ed. (Oxford University Press, Oxford, 1959).

[91] R. K. M. Thambynayagam, *The Diffusion Handbook: Applied Solutions for Engineers* (McGraw-Hill Education, New York, 2011).

[92] There was a misprint in Eq. (A7) of Ref. [54]: the minus sign in front of the last term should be replaced by a plus sign, as in our Eq. (75).

[93] D. S. Grebenkov, Probability distribution of the boundary local time of reflected Brownian motion in Euclidean domains, Phys. Rev. E **100**, 062110 (2019).

[94] D. S. Grebenkov, Residence times and other functionals of reflected Brownian motion, Phys. Rev. E **76**, 041139 (2007).

[95] D. S. Grebenkov, Statistics of diffusive encounters with a small target: Three complementary approaches, J. Stat. Mech. (2022) 083205.